JEM Journal of Experimental Medicine

ARTICLE

TGF-β signaling controls *Foxp3* methylation and T reg cell differentiation by modulating Uhrf1 activity

Xiang Sun[1*], Yu Cui[1*], Haiyun Feng[2], Haifeng Liu[1], and Xiaolong Liu[1,2]

Regulatory T (T reg) cells are required for the maintenance of immune homeostasis. Both TGF-β signaling and epigenetic modifications are important for *Foxp3* induction, but how TGF-β signaling participates in the epigenetic regulation of Foxp3 remains largely unknown. Here we showed that T cell–specific ablation of Uhrf1 resulted in T reg–biased differentiation in TCR-stimulated naive T cells in the absence of TGF-β signaling, and these Foxp3$^+$ T cells had a suppressive function. Adoptive transfer of *Uhrf1*$^{-/-}$ naive T cells could significantly suppress colitis due to increased iT reg cell generation. Mechanistically, Uhrf1 was induced upon TCR stimulation and participated in the maintenance of DNA methylation patterns of T reg cell–specific genes during cell division, while it was phosphorylated upon TGF-β stimulation and sequestered outside the nucleus, and ultimately underwent proteasome-dependent degradation. Collectively, our study reveals a novel epigenetic mechanism of TGF-β–mediated iT reg cell differentiation by modulating Uhrf1 activity and suggests that Uhrf1 may be a potential therapeutic target in inflammatory diseases for generating stable iT reg cells.

Introduction

Regulatory T (T reg) cells maintain immune system homeostasis by keeping a delicate balance between activation and suppression (Johanns et al., 2010; Dias et al., 2017). T reg cells can differentiate in the thymus and migrate to peripheral tissues as natural T reg (nT reg) cells (Curotto de Lafaille and Lafaille, 2009). In addition, induced T reg (iT reg) cells differentiate from naive CD4$^+$ T cells in the periphery under a variety of conditions (Workman et al., 2009; Bilate and Lafaille, 2012). Although they have different gene expression and epigenetic patterns (Haribhai et al., 2011), both types of T reg cell express the master transcription factor Foxp3 (Chen et al., 2011). Continuous expression of Foxp3 maintains full T reg cell suppressive capacity (Williams and Rudensky, 2007), and Foxp3 is sufficient to confer T reg cell–like suppressive function in conventional T cells by ectopic expression (Fontenot et al., 2003; Hori et al., 2003). Thus, Foxp3 is crucial for T reg cell differentiation and inhibitory function (Williams and Rudensky, 2007; Lee and Lee, 2018).

Epigenetic modifications regulate gene expression in a heritable manner without affecting genomic sequences (Trerotola et al., 2015). DNA methylation is the most well-established form of epigenetic regulation in T reg cell differentiation and controls gene expression, which is mediated by DNA methyltransferases, such as Dnmt1 and Dnmt3a/b (Liang et al., 2002; Razin and Kantor, 2005; Chen et al., 2011). It has been demonstrated that regulation of DNA methylation is indispensable for Foxp3 expression, lineage determination, and the maintenance of T reg cells (Kim and Leonard, 2007; Ohkura et al., 2013; Huehn and Beyer, 2015). Within the *Foxp3* locus, a proximal promoter and three intronic enhancers that are designated as conserved noncoding sequences (CNSs) are the primary targets of epigenetic regulation and are essential for modulating its expression (Kim and Leonard, 2007; Huehn and Beyer, 2015). The *Foxp3* promoter CpG motifs are almost completely demethylated in both nT reg cells and iT reg cells, while conventional CD4$^+$ T cells have much heavier methylation in the promoter region (Zheng et al., 2010; Huehn and Beyer, 2015). CNS2 contains CpG islands that are highly demethylated only in committed T reg cells, and demethylation of this region is required for stable expression of Foxp3 (Floess et al., 2007; Wieczorek et al., 2009; Yue et al., 2016; Someya et al., 2017).

TGF-β signaling has essential roles in the transcriptional regulation of Foxp3 expression and T reg cell suppressive function (Chen et al., 2003; Marie et al., 2005; Tone et al., 2008). Smad2 and Smad3 are phosphorylated and activated by TGF-β and can subsequently form a heterotrimer with

[1]State Key Laboratory of Cell Biology, Chinese Academy of Sciences Center for Excellence in Molecular Cell Science, Shanghai Institute of Biochemistry and Cell Biology, Chinese Academy of Sciences, University of Chinese Academy of Sciences, Shanghai, China; [2]School of Life Science and Technology, ShanghaiTech University, Shanghai, China.

*X. Sun and Y. Cui contributed equally to this paper; Correspondence to Xiaolong Liu: liux@sibs.ac.cn.

Smad4 (Souchelnytskyi et al., 1997; Derynck and Zhang, 2003). This heterotrimer binds to CNS1 in the *Foxp3* locus, which is essential for initiation of Foxp3 expression, and thus promotes T reg cell phenotype acquisition in peripheral tissues and in vitro (Schlenner et al., 2012; Kanamori et al., 2016). Continuous exposure to TGF-β can prevent the loss of Foxp3 expression in iT reg cells (Selvaraj and Geiger, 2007). However, how TGF-β signaling and epigenetic modifications are coordinated to induce Foxp3 expression has not been fully clarified.

Uhrf1 is an important epigenetic regulator that contains multiple domains, which enables it to participate in various molecular processes (Bostick et al., 2007; Liang et al., 2015; Tian et al., 2015; Kent et al., 2016; Zhao et al., 2017). Among these processes, Uhrf1 is considered to play an important role in the maintenance of DNA methylation and repression of gene expression (Sharif et al., 2007; Chen et al., 2018). During DNA replication, Uhrf1 binds methylated and hemi-methylated DNA via the SET- and RING-associated domain and recruits Dnmt1 to ensure accurate transmission of DNA methylation patterns (Liu et al., 2013). Recent studies have revealed that aberrant Uhrf1 expression is relevant to many different human malignancies and promotes cancer progression (Mudbhary et al., 2014; Sidhu and Capalash, 2017). T cell development and function involve multiple rounds of proliferation (Au-Yeung et al., 2014; Chen et al., 2015), and Uhrf1 is essential for the maintenance of DNA methylation during DNA replication, but the role of Uhrf1 in T cell development and function remains to be further investigated.

Here, we found that Uhrf1 is significantly up-regulated upon TCR stimulation. T cell–specific ablation of Uhrf1 leads to T reg cell–biased differentiation in naive $CD4^+$ T cells, with DNA hypomethylation upon TCR stimulation. Uhrf1 maintains *Foxp3* DNA methylation by recruiting Dnmt1 during cell division induced by TCR stimulation. Further analysis in WT iT reg cells revealed that Uhrf1 is sequestered in the cytoplasm through phosphorylation and undergoes subsequent proteasome-dependent degradation in response to TGF-β signaling, hence increasing Foxp3 passive demethylation and expression. Altogether, our study demonstrates a critical role of Uhrf1 in orchestrating DNA methylation, TGF-β signaling, and Foxp3 induction.

Results

Uhrf1 deficiency leads to DNA hypomethylation and T reg cell–biased transcriptome

To understand the function of Uhrf1 in T cells, we generated *Cd4*-Cre–mediated *Uhrf1* conditional knockout mice ($Uhrf1^{-/-}$ mice), and Uhrf1 was efficiently ablated from T cells (Fig. S1 A). Our recent findings suggested that Uhrf1 is required for invariant natural killer T cell development (Cui et al., 2016). Therefore, in this study, we investigated how Uhrf1 functions in conventional T cells. Unexpectedly, the overall composition of conventional T cell subsets and T cell activation showed no evident differences after Uhrf1 deletion (Fig. S1, B–D).

As Uhrf1 functions during cell proliferation and TCR stimulation drives the activation and proliferation of naive T cells, we measured Uhrf1 expression in naive T cells before and after proliferation upon TCR stimulation. Both Uhrf1 mRNA and protein levels were significantly increased after TCR stimulation (Fig. 1, A and B). RNA-sequencing (RNA-seq) analysis was performed to evaluate the roles of Uhrf1 in TCR-stimulated naive T cells. Genes involved in the immune response and immune system processes were significantly enriched in $Uhrf1^{-/-}$ naive T cells according to gene ontology (GO) enrichment analysis (Fig. S1 E). Interestingly, genes encoding molecules associated with T reg cells (e.g., *Il2ra*, *Foxp3*, *Gzmb*, and *Tnfrsf4*) were most significantly up-regulated among all 826 differentially expressed genes (Fig. 1 C). We then selected signature genes specific for T helper (Th) cells or T reg cells and found that $Uhrf1^{-/-}$ naive T cells seemed to attain a T reg cell phenotype, with higher expression of T reg cell signature genes, after TCR stimulation, which was further confirmed by real-time PCR analysis (Fig. 1, D and E). To investigate the DNA methylome changes of naive T cells after Uhrf1 deficiency, we performed whole-genome bisulfite sequencing (WGBS). Consistent with the RNA-seq data, genes involved in T reg cell differentiation were moderately enriched in $Uhrf1^{-/-}$ naive T cells according to the GO enrichment analysis in the regulation of T cell differentiation category (Fig. S1 F). Gene methylation profiles showed that T reg cell–specific genes were hypomethylated in $Uhrf1^{-/-}$ naive T cells upon TCR stimulation (Fig. 1 F). These data suggested that the DNA methylation pattern was altered, and naive T cells showed a T reg cell–biased transcriptome in $Uhrf1^{-/-}$ naive T cells upon TCR stimulation.

Uhrf1-deficient T reg cells can be induced in the absence of TGF-β signaling

To assess the role of Uhrf1 in T reg cell development, we first analyzed T reg cell differentiation in $Uhrf1^{-/-}$ mice. The proportion of T reg cell was not enhanced in the thymus, spleen, or lymph nodes of $Uhrf1^{-/-}$ mice compared with WT littermates (Fig. S1 G). Next, we cultured naive T cells from WT and $Uhrf1^{-/-}$ mice under iT reg cell skewing conditions, and no significant increase in iT reg cell differentiation was observed in $Uhrf1^{-/-}$ mice (Fig. 2 A). As both $Uhrf1^{-/-}$ and WT iT reg cells were induced up to 98%, we speculated that the difference might be obscured by TGF-β saturation. Therefore, a TGF-β concentration titration assay was performed, and as predicted, more iT reg cells were induced from $Uhrf1^{-/-}$ naive T cells with decreasing doses of TGF-β (Fig. 2 B). An explanation could be that $Uhrf1^{-/-}$ naive T cells have enhanced sensitivity to TGF-β stimulation at lower doses of TGF-β. To test this possibility, we measured the expression of TGF-β receptors (TβR) I and II and the level of phosphorylated Smad2/3 protein, and there was no substantial difference (Fig. 2 C and Fig. S2, A–C). Based on this observation and the aforementioned T reg cell–biased transcriptome in $Uhrf1^{-/-}$ naive T cells, we hypothesized that Uhrf1 deletion might induce T reg cell differentiation in the absence of TGF-β signaling. To test this hypothesis, we cultured naive T cells with TCR stimulation alone and found significantly enhanced induction of Foxp3 expression in $Uhrf1^{-/-}$ naive T cells compared with WT naive T cells (Fig. 2, D and E). In addition, cytokine production showed no significant difference after TCR stimulation,

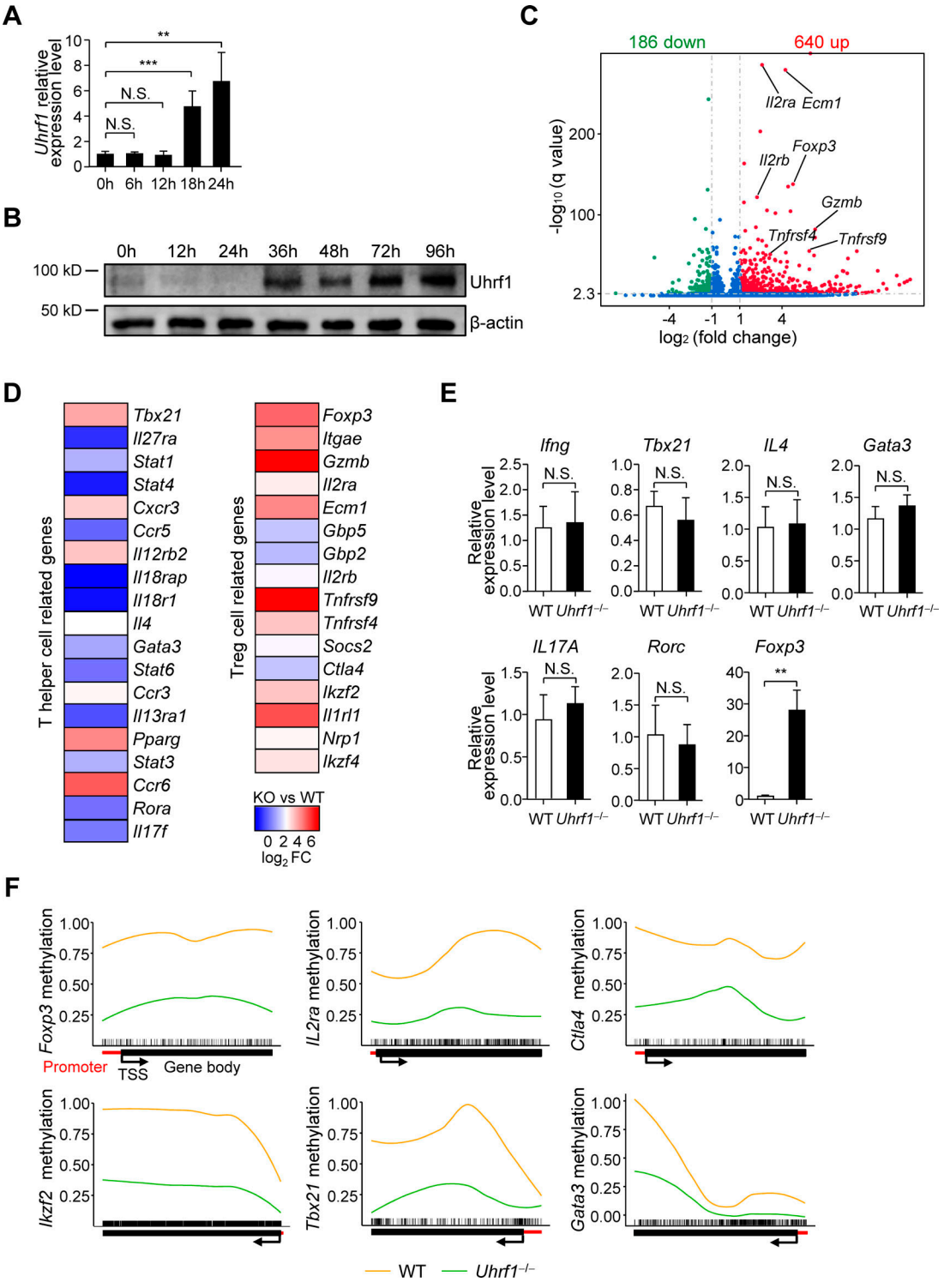

Figure 1. **Uhrf1 deficiency leads to DNA hypomethylation and T reg cell–biased transcriptome. (A)** *Uhrf1* mRNA levels in WT naive T cells stimulated with anti-CD3 plus anti-CD28 for the indicated times (n = 3). **(B)** Immunoblot analysis of Uhrf1 in WT naive T cells stimulated with anti-CD3 plus anti-CD28 for the indicated times. **(C)** RNA-seq analysis of WT and *Uhrf1*$^{-/-}$ naive T cells after 72 h of TCR stimulation. Plot shows a comparison of genes expressed in *Uhrf1*$^{-/-}$ naive T cells versus WT naive T cells. Genes significantly up-regulated (fold change >2.0) are shown in red; genes significantly down-regulated (fold change >2.0) are shown in green. An adjusted P value (q value) of 0.005 was used for the significance cutoff. **(D)** Heat map of the $\log_2$ fold change in the expression of T cell subsets signature genes. Red and blue represent high and low levels of expression of the indicated genes, respectively. **(E)** Signature gene mRNA levels in naive T cells from WT and *Uhrf1*$^{-/-}$ mice stimulated with anti-CD3 plus anti-CD28 for 72 h (n = 4). **(F)** Methylation profiles of genes encoding products known to be related to T reg and Th cell function in naive T cells from WT and *Uhrf1*$^{-/-}$ mice upon TCR stimulation, presented as values ranging from 0 (unmethylated) to 1 (methylated); below the plots, gene diagrams, showing gene body (black bars), annotated promoter region (red bar), location of individual CpG sites (tick marks) and gene direction (arrow) are presented. All data are shown as means ± SD; for all panels, **, P < 0.01, ***, P < 0.001 by Student's t test; N.S., no significance. All data are representative of or combined from at least three independent experiments. FC, fold change for gene expression; TSS, transcription start site.

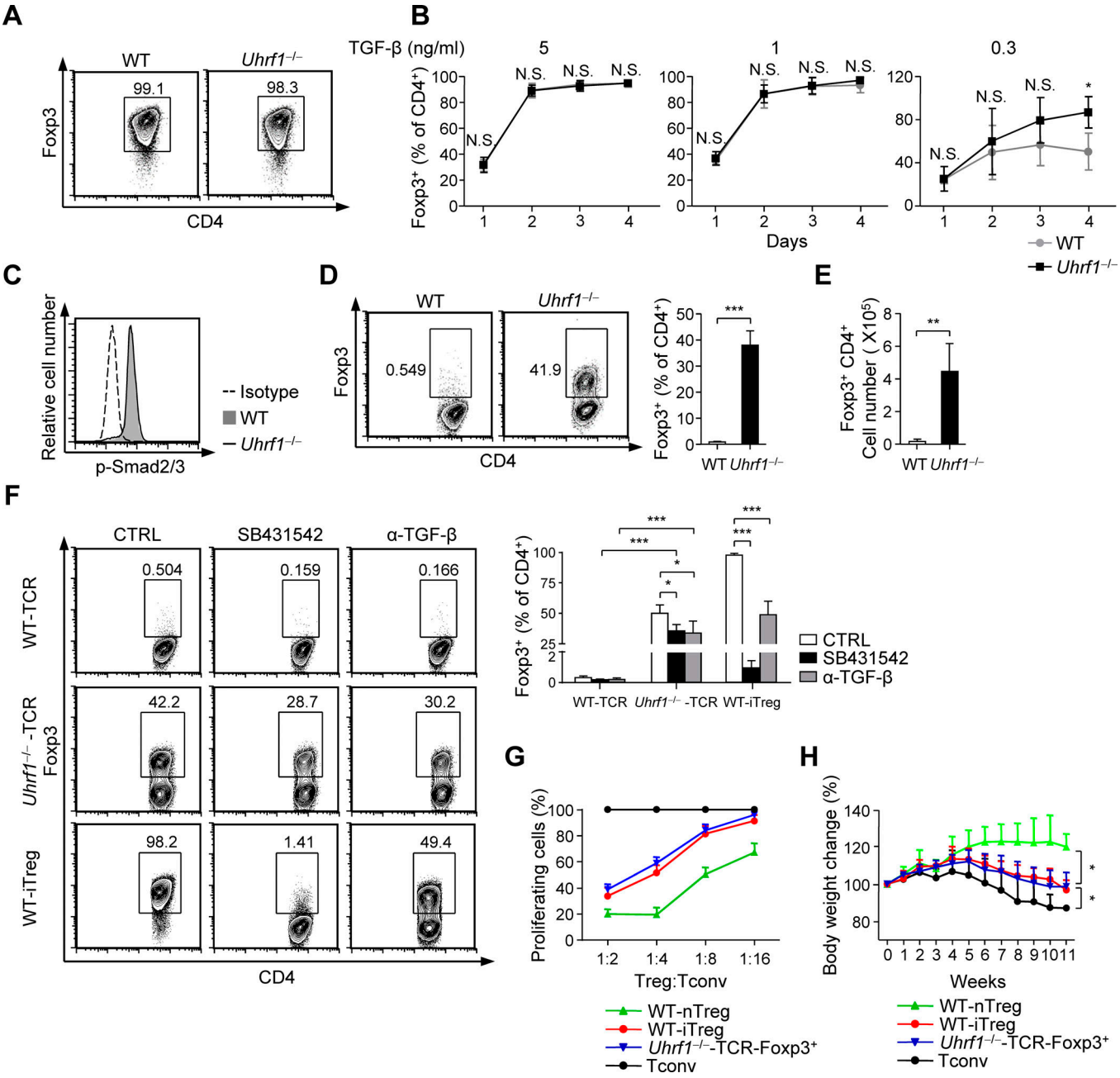

Figure 2. **Uhrf1-deficient T reg cells can be induced in the absence of TGF-β signaling. (A)** Flow-cytometric analysis of Foxp3 expression in WT and *Uhrf1*$^{-/-}$ naive T cells stimulated with anti-CD3 plus anti-CD28 in the presence of 10 ng/ml IL-2 and 10 ng/ml TGF-β for 4 d. **(B)** Foxp3 frequency of WT and *Uhrf1*$^{-/-}$ naive T cells stimulated with anti-CD3 plus anti-CD28 in the presence of 10 ng/ml IL-2 and titrated concentration of TGF-β for 1–4 d (n = 4). **(C)** Flow-cytometric analysis of phosphorylated Smad2/3 in WT and *Uhrf1*$^{-/-}$ naive T cells stimulated with anti-CD3 plus anti-CD28 in the presence of 10 ng/ml IL-2 and 0.3 ng/ml TGF-β. **(D and E)** Frequency (D) and absolute number (E) of Foxp3$^+$CD4$^+$ T cells from WT and *Uhrf1*$^{-/-}$ naive T cells stimulated with anti-CD3 plus anti-CD28 for 4 d (n = 4 or 5). **(F)** Flow-cytometric analysis of Foxp3 expression in WT and *Uhrf1*$^{-/-}$ naive T cells stimulated with anti-CD3 plus anti-CD28 or cultured under iT reg skewing conditions, in the presence or absence of 10 µg/ml neutralized TGF-β antibody or SB431542 (5 µM) for 4 d in comparison to vehicle controls (CTRL). Frequency of Foxp3$^+$CD4$^+$ T cells was quantified (n = 3). **(G)** In vitro suppression assay with CFSE-labeled naive CD4$^+$ CD25$^-$CD45RB^{high} cells from CD45.1 mice as responder cells and WT nT reg cells (CD4$^+$GFP$^+$), WT iT reg cells (CD4$^+$GFP$^+$), or stimulated (anti-CD3 and anti-CD28) *Uhrf1*$^{-/-}$ Foxp3$^+$ T cells (CD4$^+$GFP$^+$) were isolated as T reg cells. Ratios of responder cells with more than one division are presented (n = 3). **(H)** Body weight of *Rag1*$^{-/-}$ mice injected with sorted naive CD4$^+$CD25$^-$CD45RB^{high} T cells from CD45.1$^+$ mice alone or in combination with WT nT reg cells (CD4$^+$GFP$^+$), WT iT reg cells (CD4$^+$GFP$^+$), or stimulated (anti-CD3 and anti-CD28) *Uhrf1*$^{-/-}$ Foxp3$^+$ T cells (CD4$^+$GFP$^+$; n = 7–12 for each cell type for each week). All data are shown as means ± SD; for all panels, *, P < 0.05, ** P < 0.01, ***, P < 0.001 by Student's t test; N.S., no significance. All data are representative of or combined from at least three independent experiments. T conv, conventional T cell.

which was consistent with the RNA-seq data and confirmed the T reg cell–biased differentiation and special regulation of Foxp3 in *Uhrf1*$^{-/-}$ T cells upon TCR stimulation (Fig. S2 D). To better clarify the role of TGF-β signaling on Foxp3 induction in TCR-stimulated *Uhrf1*$^{-/-}$ T cells, we blocked TGF-β signaling by using either a neutralizing TGF-β antibody or an inhibitor of TGF-β receptor (SB431542), and the induction of Foxp3 in *Uhrf1*$^{-/-}$ naive T cells was still notably elevated in the absence of TGF-β signaling compared with corresponding WT controls, although slightly decreased compared with vehicle-treated *Uhrf1*$^{-/-}$ T cells (Fig. 2 F). Thus, *Uhrf1*$^{-/-}$ naive T cells could initiate Foxp3 expression without TGF-β signaling.

To functionally characterize Foxp3^{+} T cells induced from *Uhrf1*$^{-/-}$ naive T cells, we crossed *Uhrf1*$^{-/-}$ or WT mice with Foxp3^{EGFP} mice to mark Foxp3^{+} T cells with an enhanced green fluorescent protein (EGFP) reporter, isolated CD4^{+}EGFP^{+} T cells, and performed an in vitro suppression assay. *Uhrf1*$^{-/-}$ Foxp3^{+} T cells suppressed conventional T cell proliferation as effectively as WT iT reg cells, though less effectively than WT nT reg cells (Fig. 2 G). To further investigate the function of *Uhrf1*$^{-/-}$ Foxp3^{+} T cells in vivo, we induced colitis by adoptive transfer of naive T cells from CD45.1 mice together with TCR-stimulated CD4^{+}EGFP^{+} cells from Foxp3^{EGFP} *Uhrf1*$^{-/-}$ mice, Foxp3^{EGFP} WT iT reg cells, or Foxp3^{EGFP} WT nT reg cells into *Rag1*$^{-/-}$ mice, and the suppressive capacity was similar to that observed in the in vitro suppression assay (Fig. 2 H). Taken together, these findings demonstrated that *Uhrf1*$^{-/-}$ naive T cells could differentiate into functional T reg cells in the absence of TGF-β signaling.

Uhrf1-deficient naive T cells suppress colitis due to increased frequency of in vivo–generated iT reg cells

To further evaluate the importance of Uhrf1-mediated regulation of CD4^{+} T cell differentiation under pathophysiological conditions in vivo, we examined the *Uhrf1*$^{-/-}$ naive T cell phenotype in a T cell transfer model of colitis and excluded the influence of *Uhrf1*$^{-/-}$ invariant natural killer T cells. I.v. injection of *Rag1*$^{-/-}$ mice with *Uhrf1*$^{-/-}$ naive T cells failed to induce colitis, with no obvious body weight loss in the mice (Fig. 3 A). Gross examination of the colon did not show enlargement or thickening as observed in WT naive T cell–transferred mice, and H&E staining of colon tissues indicated a disruption of epithelial damage, with massive infiltration of leukocytes in WT but not *Uhrf1*$^{-/-}$ naive T cell–transferred mice (Fig. 3, B and C). The differentiation of the transferred naive T cells was analyzed, and a significant increase in iT reg cell generation from *Uhrf1*$^{-/-}$ naive T cells was observed, which was consistent with the in vitro results (Fig. 3 D). As previously reported, the proinflammatory cytokines IFN-γ and IL-17A produced from Th1 and Th17 cells, respectively, are major contributors to inflammatory bowel disease. Flow-cytometric analysis of cytokines recovered from colon lamina propria lymphocytes (cLPs), mesenteric lymph nodes (MLNs), and spleen of *Rag1*$^{-/-}$ mice revealed that *Uhrf1*$^{-/-}$ naive T cells produced less IFN-γ and IL-17A than WT naive T cells (Fig. 3 E).

To investigate whether Uhrf1 deletion might affect Th1 and Th17 cell differentiation and lead to the ameliorated colitis, in vitro effector T cell differentiation experiments were performed, and no significant difference was observed between WT and *Uhrf1*$^{-/-}$ T cells (Fig. S2 E). Given that *Uhrf1*$^{-/-}$ T cells could induce T reg cells after TCR stimulation in the absence of TGF-β, the other possibility was that the T reg cell–biased differentiation in *Uhrf1*$^{-/-}$ naive T cells might inhibit Th1 and Th17 cell differentiation potential. Indeed, after TCR stimulation of WT and *Uhrf1*$^{-/-}$ naive T cells for 2 d, further Th1 and Th17 cell differentiation showed significantly less IFN-γ and IL-17A production from *Uhrf1*$^{-/-}$ effector T cells compared with WT effector T cells (Fig. S2 F). Collectively, these data suggested that *Uhrf1*$^{-/-}$ naive T cells were more prone to induce iT reg cells under pathophysiological conditions, which suppressed proinflammatory cytokine production and ameliorated colitis.

Uhrf1 is required for the maintenance of *Foxp3* DNA methylation during cell proliferation

Given that Uhrf1 is induced by TCR stimulation and that DNA methylation patterns are established during cell division, we wondered whether the maintenance of *Foxp3* methylation relies on Uhrf1 and cell division. To this end, naive T cells from WT and *Uhrf1*$^{-/-}$ mice were stimulated via TCR for different times. As the culture time increased, DNA methylation levels of CpG islands in the promoter and CNS2 region of the *Foxp3* gene decreased, and more T reg cells were induced in *Uhrf1*$^{-/-}$ T cells (Fig. S3, A and B). In addition, blockade of TGF-β signaling did not alter the *Foxp3* DNA methylation pattern when Uhrf1 was deleted (Fig. S3 C), which was consistent with Foxp3 expression shown in Fig. 2 F and confirmed the induction of *Uhrf1*$^{-/-}$ T reg cells without TGF-β signaling. These results demonstrated that Uhrf1 maintained *Foxp3* DNA methylation to restrict its expression during TCR stimulation.

To further clarify the relationship between the maintenance of *Foxp3* DNA methylation and cell proliferation, we analyzed the pattern of Foxp3 expression versus cell division at designated time points. The proportion of CD4^{+}Foxp3^{+} T cells in *Uhrf1*$^{-/-}$ T cells continued to increase in each successive generation, while the proportion of WT T cells was stable at low levels, with even slightly lower levels after cell division (Fig. 4, A and B). Consistent with a Foxp3 expression pattern, the DNA methylation level of *Uhrf1*$^{-/-}$ T cells was reduced in each successive generation, suggesting that Uhrf1-mediated *Foxp3* DNA methylation depended on cell division (Fig. 4 C). We next investigated whether entry into the cell cycle was required to induce Foxp3 expression in *Uhrf1*$^{-/-}$ naive T cells upon TCR stimulation. After cell cycle arrest, *Uhrf1*$^{-/-}$ naive T cells were barely able to induce Foxp3^{+} cells, and the *Foxp3* locus showed similar DNA methylation patterns to those of WT controls (Fig. 4, D and E). In addition, *Foxp3* mRNA levels were comparable upon TCR stimulation between *Uhrf1*$^{-/-}$ and WT naive T cells before T cells were divided (Fig. S3 D). Furthermore, we found that WT iT reg cells were harder to induce after cell cycle arrest (Fig. S3 E). Therefore, cell division was necessary for Uhrf1 to maintain *Foxp3* DNA methylation and subsequently restrict Foxp3 expression.

Next, we wanted to test whether Uhrf1 maintains *Foxp3* DNA methylation by recruiting Dnmt1 during T cell

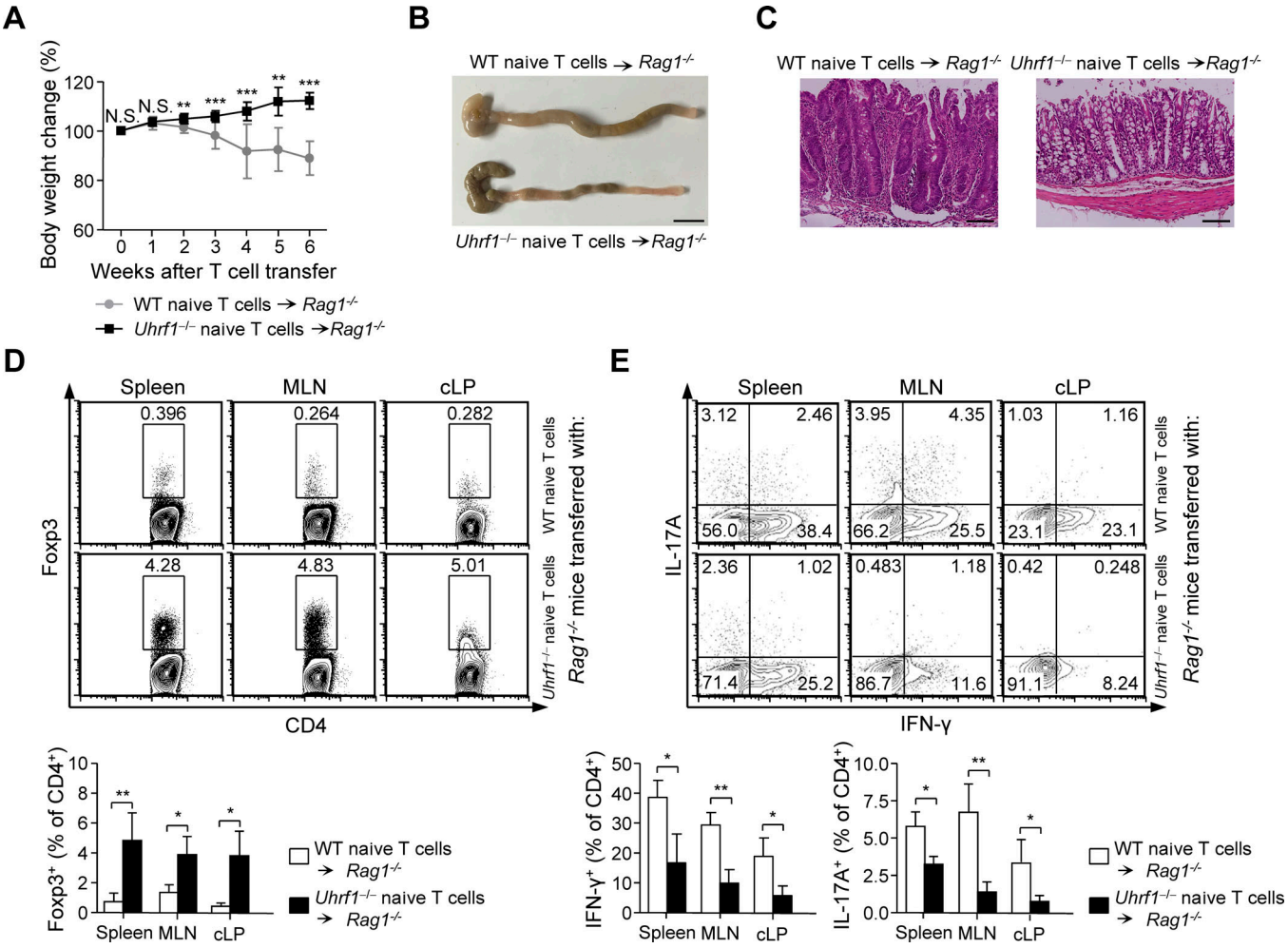

Figure 3. **Uhrf1-deficient naive T cells suppress colitis due to increased frequency of in vivo–generated iT reg cells. (A)** Body weights of *Rag1*$^{-/-}$ mice injected with sorted naive CD4^{+}CD25^{-}CD45RB^{high} T cells from WT and *Uhrf1*$^{-/-}$ mice were monitored for 6 wk after the injection. Body weight percentages relative to the respective preinjection values were calculated every week (n = 4–7 for each cell type for each week). **(B)** Colon tissues of *Rag1*$^{-/-}$ mice injected with naive T cells as shown in A. Morphology of the representative colon tissue is shown. Scale bars, 1 cm. **(C)** H&E staining of colon sections from *Rag1*$^{-/-}$ mice transferred with the indicated cells, as shown in A. Scale bar, 100 µm. **(D)** Flow-cytometric analysis of Foxp3 expression in transferred CD4^{+} T cells recovered from cLP, MLN, and spleen in *Rag1*$^{-/-}$ recipients. Frequency of Foxp3^{+}CD4^{+} T cells was quantified (n = 3–5). **(E)** Flow-cytometric analysis of IFN-γ and IL-17A production in transferred CD4^{+} T cells recovered from cLP, MLN, and spleen in *Rag1*$^{-/-}$ recipients. Frequency of IFN-γ^{+}CD4^{+} and IL-17A^{+}CD4^{+} T cells was quantified (n = 3–5). All data are shown as means ± SD; for all panels, *, P < 0.05, **, P < 0.01, ***, P < 0.001 by Student's t test; N.S., no significance. All data are representative of or combined from at least three independent experiments.

stimulation. As expected, TCR stimulation–induced interaction between Uhrf1 and Dnmt1 was observed in WT CD4^{+} T cells (Fig. S3 F). Chromatin immunoprecipitation (ChIP) experiments with anti-Dnmt1 antibody revealed that Dnmt1 was enriched at the promoter and CNS2 region of the *Foxp3* locus and that Uhrf1 deficiency suppressed this enrichment (Fig. 4 F). Furthermore, we used the H346G Uhrf1 mutant to interrupt the targeting of Dnmt1 to replication foci (Qin et al., 2015), and analyzed Foxp3 expression. Retroviral expression of H346G Uhrf1 mutant did not "rescue" the reduced Foxp3 induction and increased DNA methylation level observed in *Uhrf1* retrovirus-transduced cells (Fig. S3, G and H). These results indicated the involvement of Uhrf1 in regulating *Foxp3* DNA methylation not only after TCR stimulation but also in iT reg cell differentiation during cell proliferation.

TGF-β induces Uhrf1 phosphorylation and sequesters Uhrf1 in the cytoplasm

Many definitive studies have uncovered the essential role of TGF-β signaling in the initiation and transcriptional regulation of Foxp3 expression. Our aforementioned data demonstrated that *Uhrf1*$^{-/-}$ naive T cells can induce Foxp3 expression in the absence of TGF-β signaling. These findings prompted us to hypothesize that TGF-β signaling might initiate Foxp3 expression by reversing the Uhrf1-mediated maintenance of DNA methylation. As most functions ascribed to Uhrf1 occur in the nucleus, we first examined whether TGF-β induced Foxp3 expression by modulating the localization of Uhrf1. Immunofluorescence analysis confirmed the specificity of our homemade Uhrf1 antibody (Fig. S4 A). Notably, the retention of Uhrf1 in the cytoplasm was significantly increased after TGF-β treatment, which was further confirmed by immunoblot analysis (Fig. 5, A and B;

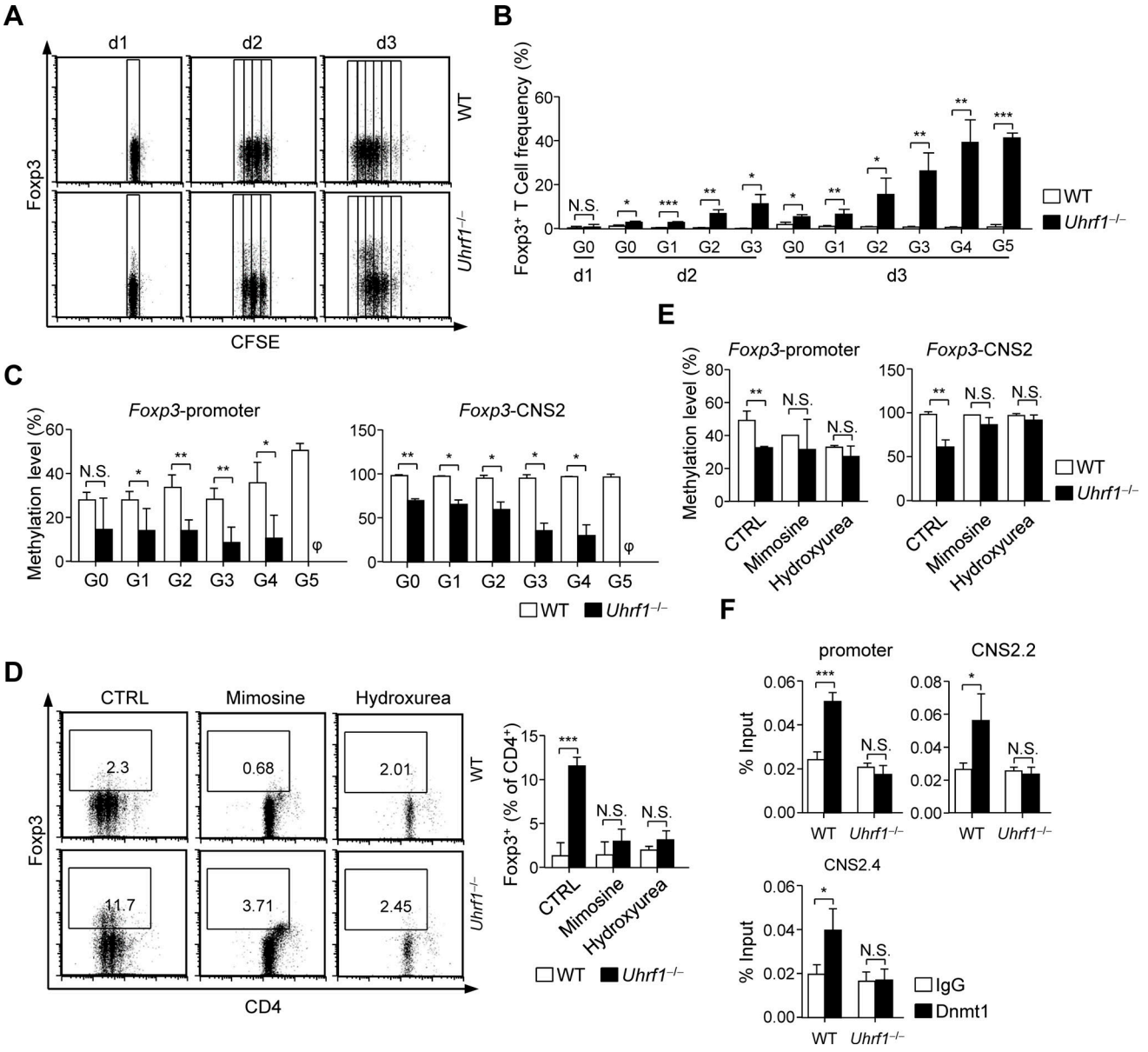

Figure 4. **Uhrf1 is required for the maintenance of Foxp3 DNA methylation during cell proliferation. (A)** Flow-cytometric analysis of CFSE-labeled naive T cells from WT and *Uhrf1*$^{-/-}$ mice treated with anti-CD3 plus anti-CD28 for 1–3 d. A pane represents one cell generation. **(B)** The percentage of Foxp3^{+}CD4^{+} T cells in each generation from WT and *Uhrf1*$^{-/-}$ mice as shown in A (n = 3 or 4 for each generation). **(C)** The methylation levels of the *Foxp3* gene at the promoter and CNS2 region by bisulfite sequencing in each generation at day 3 in A (n = 3 or 4). φ, not enough cells for analysis. **(D)** Flow-cytometric analysis of Foxp3 expression in WT and *Uhrf1*$^{-/-}$ naive T cells stimulated with anti-CD3 plus anti-CD28 in the presence of cell cycle inhibitors: mimosine (300 µM) and hydroxurea (200 µM) for 3 d in comparison to vehicle controls (CTRL). Frequency of Foxp3^{+}CD4^{+} T cells was quantified (n = 3 or 4). **(E)** Percentages of CpG island methylation at the *Foxp3* promoter and CNS2 region determined by bisulfite sequencing in WT and *Uhrf1*$^{-/-}$ naive T cells stimulated as described in D (n = 3). **(F)** ChIP assay of Dnmt1 in the *Foxp3* promoter and CNS2 regions in WT and *Uhrf1*$^{-/-}$ naive T cells treated with anti-CD3 plus anti-CD28 for 4 d. Cell lysates were immunoprecipitated with anti-Dnmt1 (filled bars) or control IgG (open bars; n = 3). All data are shown as means ± SD; for all panels, *, P < 0.05, **, P < 0.01, ***, P < 0.001 by Student's t test; N.S., no significance. All data are representative of or combined from at least three independent experiments. CTRL, control.

and Fig. S4 B). Accordingly, the DNA methylation level of the *Foxp3* locus was decreased (Fig. 5 C). These results indicated that TGF-β signaling might sequester Uhrf1 in the cytoplasm, which resulted in decreased DNA methylation of *Foxp3* locus.

It was reported that protein phosphorylation could have either an enhancing or an inhibitory effect on nuclear translocation (Nardozzi et al., 2010). To determine whether phosphorylation is required for the change in Uhrf1 localization during iT reg cell differentiation, we first measured Uhrf1 phosphorylation in WT naive T cells after TGF-β treatment. Total serine phosphorylation of Uhrf1 was noticeably up-regulated after culture with TGF-β for 2 d (Fig. 5 D). Next, we treated cells with roscovitine, a known inhibitor of cyclin-dependent kinases that has been reported to inhibit Uhrf1

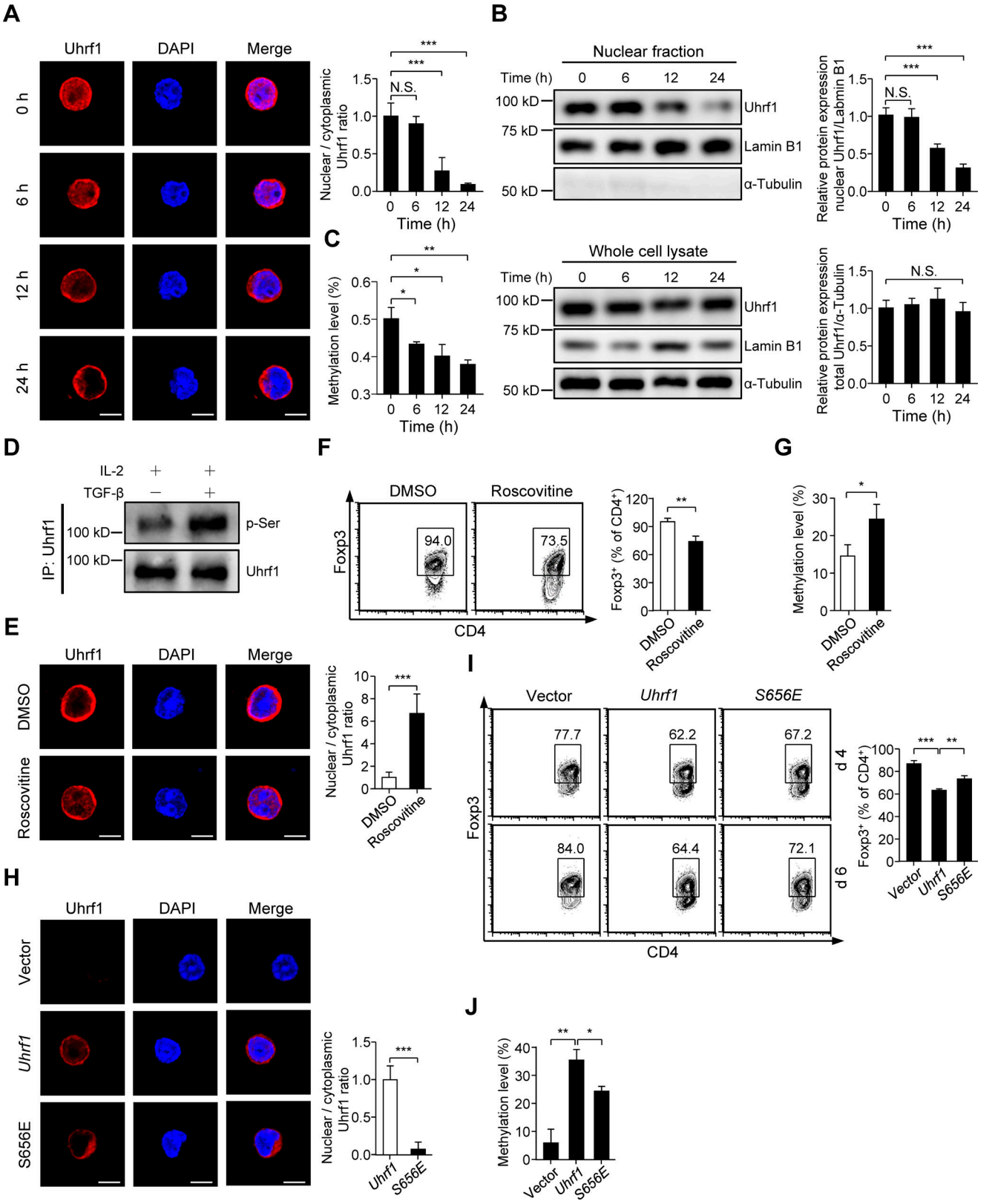

Figure 5. **TGF-β induces Uhrf1 phosphorylation and sequesters Uhrf1 in the cytoplasm. (A)** Representative confocal microscopy of the subcellular localization of endogenous Uhrf1 in WT naive T cells stimulated with anti-CD3 and anti-CD28 for 96 h, and TGF-β was added for 0 h, 6 h, 12 h, or 24 h before 96-h harvest. DNA was counterstained with DAPI. Scale bars, 5 µm. The ratio of nuclear to cytoplasmic Uhrf1 was quantified (each time point with ≥65 cells quantified). **(B)** Immunoblot analysis of Uhrf1, lamin B1, and α-tubulin in nuclear fractions or total cell lysates of naive T cells after TCR stimulation in the presence of TGF-β for the indicated times as described in A. Relative protein expression of nuclear Uhrf1 or total Uhrf1 was quantified respectively (n = 3). **(C)** The methylation levels of the *Foxp3* promoter region in naive T cells cultured as described in A (n = 3). **(D)** Immunoblot analysis of the phosphorylation

(p-Ser) of endogenous Uhrf1 in WT naive T cells stimulated with anti-CD3 and anti-CD28 or cultured under iT reg skewing conditions for 2 d. **(E)** Representative confocal microscopy of the subcellular localization of endogenous Uhrf1 in WT naive T cells cultured under iT reg skewing conditions in the presence or absence of roscovitine (10 µM) for 2 d before 4-d harvest. DNA was counterstained with DAPI. Scale bars, 5 µm. The ratio of nuclear to cytoplasmic Uhrf1 was quantified (each treatment with ≥58 cells quantified). **(F)** Flow-cytometric analysis of Foxp3 expression in T cells as treated in E. Frequency of $Foxp3^+CD4^+$ T cells was quantified (n = 3). **(G)** The methylation levels of the *Foxp3* promoter region in T cells as treated in E (n = 3). **(H)** Representative confocal microscopy of the subcellular localization of endogenous Uhrf1 in $Uhrf1^{-/-}$ T cells transfected with vector, *Uhrf1*, or its mutant $Uhrf1^{S656E}$ (Ser-656 changed to a glutamic acid residue to mimic phosphorylation) and then cultured under iT reg skewing conditions for 6 d. DNA was counterstained with DAPI. Scale bars, 5 µm. The ratio of nuclear to cytoplasmic Uhrf1 was quantified (each transfected treatment with ≥60 cells quantified). **(I)** Flow-cytometric analysis of Foxp3 expression in transfected T cells, as treated in H, for 4 or 6 d. Frequency of $Foxp3^+CD4^+$ T cells for 6 d was quantified (n = 3). **(J)** The methylation levels of the *Foxp3* promoter region in transfected T cells, as treated in H (n = 3). All data are shown as means ± SD; for all panels, *, P < 0.05, **, P < 0.01, ***, P < 0.001 by Student's t test; N.S., no significance. All data are representative of or combined from at least three independent experiments. IP, immunoprecipitation.

phosphorylation (Ma et al., 2012), and analyzed Uhrf1 localization. As expected, roscovitine treatment led to prominent nuclear localization of Uhrf1, and the corresponding DNA methylation level and Foxp3 expression were increased and down-regulated, respectively (Fig. 5, E–G). A previous study suggested that phosphorylation of Uhrf1 (p-Ser-661) could change its localization in human cell lines (Chu et al., 2012). To directly examine the effect of Uhrf1 phosphorylation on its localization and Foxp3 expression, $Uhrf1^{-/-}$ naive T cells were transiently transfected with an empty vector, *Uhrf1*, or $Uhrf1^{S656E}$ and cultured under iT reg skewing conditions. After retroviral expression of S656E Uhrf1 mutant, Uhrf1 localization was exclusively cytoplasmic compared with that of *Uhrf1*-transfected T cells (Fig. 5 H). The Foxp3 methylation status and expression results were consistent with the observed changes in Uhrf1 localization (Fig. 5, I and J). Collectively, these results suggested that TGF-β signaling induced Uhrf1 phosphorylation and sequestered Uhrf1 in the cytoplasm, which reversed DNA methylation-mediated repression and consequently initiated Foxp3 expression.

Degradation of sequestered cytoplasmic Uhrf1 is regulated by Usp7 after TGF-β stimulation

We next investigated whether the alteration of Uhrf1 localization affected its protein expression after TGF-β stimulation. Indeed, the abundance of the Uhrf1 protein was observed to decrease in a dose-dependent manner after TGF-β treatment for 4 d, whereas IL-2 plus TCR or TCR stimulation alone showed no effect (Fig. 6 A and Fig. S5 A). In addition, *Uhrf1* mRNA levels had no change in T cells after TGF-β treatment (Fig. S5 B). The abundance of the Dnmt1 protein was barely altered upon TGF-β stimulation (Fig. S5 C). There are two major mechanisms by which animal cells degrade proteins: the lysosome and the proteasome (Ciechanover, 2005). Proteasome and lysosome inhibitors were used to clarify the Uhrf1 degradation mechanism. Only MG132 (a proteasome inhibitor) restored Uhrf1 expression after TGF-β treatment, and this effect was dose dependent (Fig. 6 B and Fig. S5 D). Immunoblot analysis showed that ubiquitination of Uhrf1 was enhanced in T cells after TGF-β treatment compared with that in TCR-stimulated T cells (Fig. 6 C and Fig. S5 E). These results suggested that TGF-β specifically induced proteasome-dependent degradation of Uhrf1.

Phosphorylation can serve as a marker that promotes subsequent ubiquitination, in particular when ubiquitination leads to degradation (Hunter, 2007; Nguyen et al., 2013). So we investigated the relationship between phosphorylation and ubiquitination of Uhrf1 induced by TGF-β and found that the Uhrf1 ubiquitination level was elevated, accompanied by increasing phosphorylation levels (Fig. 6 D). To evaluate whether Uhrf1 phosphorylation affected its degradation and protein abundance, we inhibited Uhrf1 phosphorylation by roscovitine and found that blocking phosphorylation significantly suppressed Uhrf1 degradation after TGF-β stimulation (Fig. 6 E). Therefore, Uhrf1 phosphorylation was required for its degradation.

To investigate which lysine residue of Uhrf1 was responsible for its ubiquitination, we analyzed endogenous ubiquitin modifications of Uhrf1 by mass spectrometry. Lys24, Lys50, Lys84, Lys172, and Lys196 of Uhrf1 were identified as sites modified by ubiquitin (Fig. S5 F). Protein half-life assays were used to confirm that Lys84, Lys172, and Lys196 were responsible for the ubiquitination of Uhrf1, based on the observation that replacing those lysine residues with arginine (K84R, K172R, and K196R) completely rescued Uhrf1 degradation (Fig. S5 G). Then, $Uhrf1^{-/-}$ naive T cells were transiently transfected with empty vector, *Uhrf1*, or $Uhrf1^{K84/172/196R}$, and iT reg cells were induced. Retroviral expression of the K84/172/196R Uhrf1 mutant restored Uhrf1 expression after TGF-β stimulation compared with that of *Uhrf1*-transfected T cells (Fig. 6 F).

To further clarify the mechanism of Uhrf1 degradation after TGF-β stimulation, mass spectrometry was performed, and the deubiquitylase Usp7 was identified, which was consistent with previous reports (Qin et al., 2011; Zhang et al., 2015; Fig. S5 H). Immunoprecipitation assays confirmed the interaction between endogenous Uhrf1 and Usp7 in WT $CD4^+$ T cells, and TGF-β attenuated this interaction (Fig. 6 G). As Usp7 is a deubiquitinase and prevents protein degradation, Uhrf1 protein abundance decreased in T cells after treatment with the Usp7 inhibitor (Fig. 6 H). We next examined whether blocking Uhrf1 degradation could inhibit iT reg cell differentiation. Intriguingly, the $Uhrf1^{K84/172/196R}$ mutant moderately inhibited Foxp3 induction to an extent similar to that of Uhrf1 (Fig. 6 I). In summary, these results indicated that TGF-β induced Uhrf1 phosphorylation and sequestered it outside the nucleus, which led to decreased *Foxp3* DNA methylation and initiation of Foxp3 expression, and cytoplasmic Uhrf1 underwent proteasome-dependent degradation through inhibition of Usp7-mediated deubiquitination as a consequence.

Passive demethylation regulates Foxp3 induction during iT reg cell differentiation

DNA methylation can be erased directly by either an active demethylation mechanism involving ten-eleven translocation (TET) proteins or a passive demethylation process through

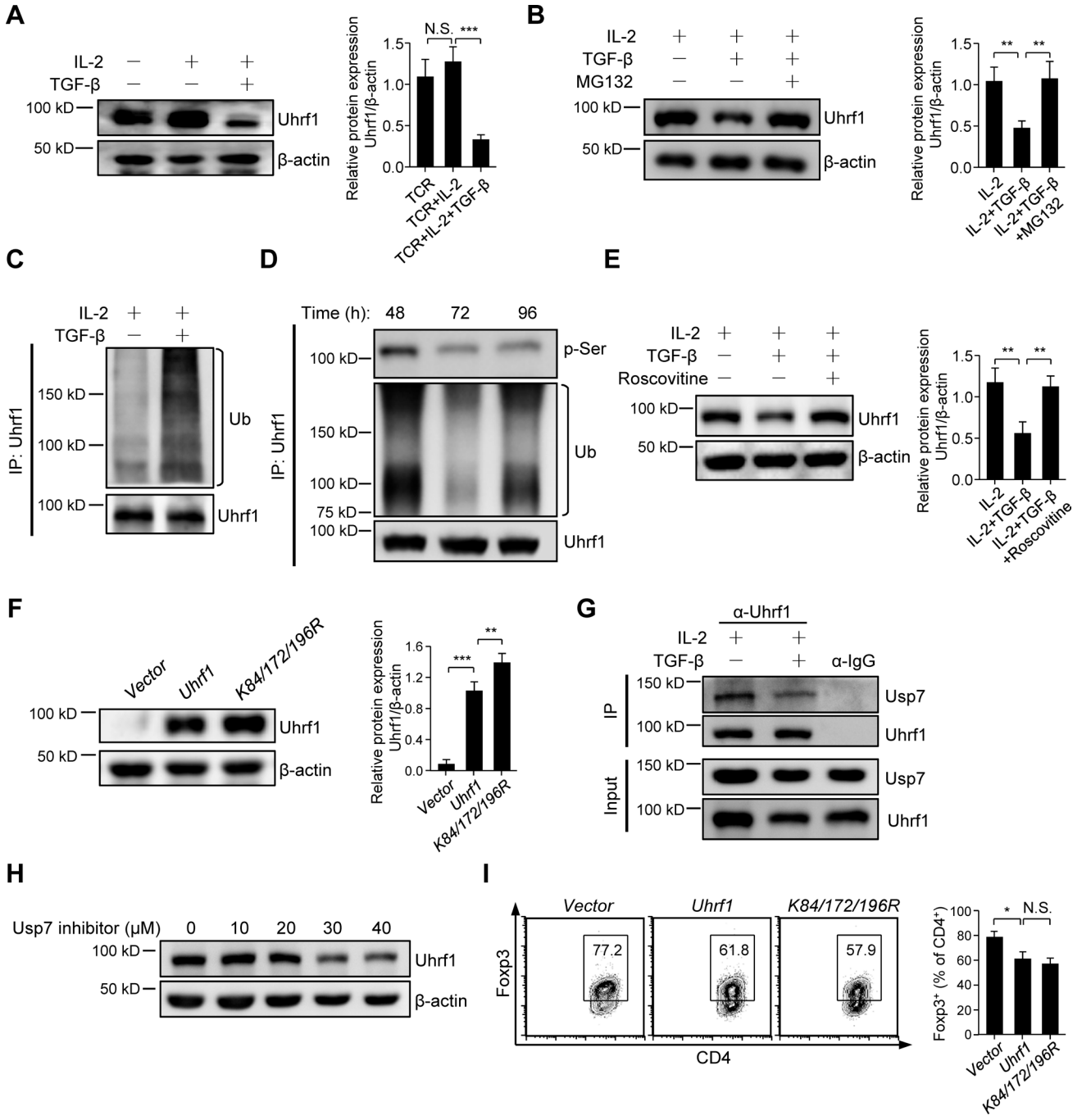

Figure 6. **Degradation of sequestered cytoplasmic Uhrf1 is regulated by Usp7 after TGF-β stimulation. (A)** Immunoblot analysis of Uhrf1 in WT naive T cells stimulated with anti-CD3 and anti-CD28 in the presence or absence of 10 ng/ml IL-2 and/or 10 ng/ml TGF-β for 4 d. **(B)** Immunoblot analysis of Uhrf1 in WT naive T cells stimulated with anti-CD3 and anti-CD28 in the presence of IL-2, IL-2 plus TGF-β, or IL-2 and TGF-β plus MG132 for 4 d. Relative protein expression of Uhrf1 was quantified (n = 3). **(C)** Immunoblot analysis of the ubiquitination (Ub) of endogenous Uhrf1 in WT naive T cells stimulated with anti-CD3 and anti-CD28 plus 10 ng/ml IL-2 in the presence or absence of 10 ng/ml TGF-β for 4 d. IP, immunoprecipitation. **(D)** Immunoblot analysis of the phosphorylation and ubiquitination of endogenous Uhrf1 in WT naive T cells cultured under iT reg skewing conditions for 48 h, 72 h, and 96 h. **(E)** Immunoblot analysis of Uhrf1 in WT naive T cells stimulated with anti-CD3 and anti-CD28 in the presence of IL-2, IL-2 plus TGF-β, or IL-2 and TGF-β plus roscovitine (10 μM) for 4 d. Relative protein expression of Uhrf1 was quantified (n = 3). **(F)** Immunoblot analysis of Uhrf1 in *Uhrf1*$^{-/-}$ T cells transfected with *Uhrf1* or its mutant *Uhrf1*$^{K84/172/196R}$ and then cultured under iT reg skewing conditions for 6 d. Relative protein expression of Uhrf1 was quantified (n = 3). **(G)** Immunoblot analysis of Usp7 immunoprecipitated by endogenous Uhrf1 in WT T cells stimulated with anti-CD3 and anti-CD28 plus 10 ng/ml IL-2 in the presence or absence of 10 ng/ml TGF-β for 4 d. **(H)** Immunoblot analysis of Uhrf1 in WT naive T cells cultured under iT reg skewing conditions in the presence or absence of Usp7 inhibitor for 4 d. **(I)** Flow-cytometric analysis of Foxp3 expression in *Uhrf1*$^{-/-}$ T cells transfected with *Uhrf1* or its mutant *Uhrf1*$^{K84/172/196R}$ and then cultured under iT reg skewing conditions for 6 d. Frequency of Foxp3$^+$CD4$^+$ T cells was quantified (n = 3). All data are shown as means ± SD; for all panels, *, P < 0.05, **, P < 0.01, ***, P < 0.001 by Student's t test; N.S., no significance. All data are representative of or combined from at least three independent experiments.

replication-coupled dilution of 5-methylcytosine (5-mC). Previous studies have shown that TET proteins mediate the loss of 5-mC in the *Foxp3* T reg cell–specific demethylated region in T reg cells (Yue et al., 2016), while our data suggested that Uhrf1 directly participated in the maintenance of *Foxp3* DNA methylation during cell division and that TGF-β signaling reversed *Foxp3* DNA methylation by modulating Uhrf1 activity. To understand the relationship between TET proteins and Uhrf1 in the modulation of *Foxp3* DNA methylation, we first measured whether Uhrf1 deletion would affect the abundance of TET proteins and found that there was no difference in TET protein levels after Uhrf1 ablation (Fig. 7 A). Vitamin C and S-2-hydroxyglutarate (S-2HG) are TET protein agonist and inhibitor, respectively (Losman et al., 2013; Yue et al., 2016). Treatment with vitamin C or S-2HG failed to alter *Foxp3* methylation pattern or expression level of *Uhrf1*$^{-/-}$ naive T cells upon TCR stimulation (Fig. 7, B–E). Thus, TET-mediated active demethylation was not involved in the induction of Foxp3 expression in *Uhrf1*$^{-/-}$ naive T cells upon TCR stimulation.

To further clarify the relationship between active and passive demethylation during Foxp3 induction, we used the bisulfite sequencing and oxidative bisulfite methods to measure the enrichment of 5-mC and 5-hydroxymethylcytosine (5-hmC) within the *Foxp3* promoter and CNS2 region during iT reg cell differentiation. The 5-mC and 5-hmC conversion efficiencies were confirmed using 5-mC and 5-hmC standard DNA. We calculated the percentage of 5-mC, 5-hmC, and C/5fC/5caC at CpGs in the promoter and CNS2 regions, respectively. In the CNS2 region, all CpGs showed progressive increase of 5-hmC following the loss of 5-mC after 48 h, which was consistent with the previously reported role of TET proteins in improving Foxp3 stability (Yue et al., 2016; Fig. 7 F). However, in the promoter region, there was moderate 5-hmC generation, but accompanied by rapidly reduced 5-mC after 24 h, C/5fC/5caC level was noticeably increased (Fig. 7 G). These results suggested that passive demethylation triggered by inhibition of Uhrf1 activity mainly functioned in the promoter region of *Foxp3* locus, while active demethylation mediated by TET proteins acted primarily in the CNS2 region during iT reg cell differentiation.

Based on the findings described above, we assumed that overexpression of Uhrf1 would increase the methylation level of the *Foxp3* promoter region. Retroviral expression of Uhrf1 in WT T cells resulted in attenuated passive demethylation, followed by higher methylation levels of the *Foxp3* promoter region and eventually less Foxp3 induction (Fig. 7, H and I). Altogether, these data supported the notion that Uhrf1 was involved in passive demethylation of the *Foxp3* promoter region and contributed to Foxp3 induction, while active demethylation of the *Foxp3* CNS2 region via TET proteins determined Foxp3 stability.

Discussion

In T reg cells, DNA demethylation has been found to be essential for *Foxp3* transcription (Lal et al., 2009), and TGF-β signaling plays a crucial role in *Foxp3* transcriptional regulation (Tone et al., 2008). However, how DNA methylation-mediated repression is reversed before *Foxp3* gene transcription is less clear. Here, we identified Uhrf1 as a DNA-methylation adaptor regulated by TGF-β signaling that controlled *Foxp3* methylation and iT reg cell differentiation. *Uhrf1*$^{-/-}$ naive T cells underwent T reg cell–biased differentiation upon TCR stimulation, and these Foxp3^{+} T cells had suppressive functions both in vitro and in vivo. Uhrf1 maintained *Foxp3* DNA methylation by recruiting Dnmt1 during cell division induced by TCR stimulation. In iT reg cells, Uhrf1 was involved in the passive demethylation of the *Foxp3* promoter region upon TGF-β stimulation, with sequential initiation of Foxp3 expression. Mechanistically, Uhrf1 was phosphorylated upon TGF-β treatment and largely excluded from the nucleus. Phosphorylated Uhrf1 underwent proteasomal degradation, and DNA methylation-mediated repression of *Foxp3* promoter region was reversed as an outcome. Taken together, our findings revealed a unique mechanism of TGF-β signaling-mediated epigenetic regulation of *Foxp3* methylation and iT reg cell differentiation, which was accomplished through modulating Uhrf1 activity.

Naive T cells are able to both proliferate and differentiate (Jelley-Gibbs et al., 2000). TCR stimulation in the absence or presence of environmental cytokines induces a network of downstream signaling pathways, which eventually lead to naive T cell proliferation or differentiation into various inflammatory effector subsets (e.g., Th1, Th2, and Th17 cells) or T reg cells (Zhou et al., 2009). However, it remains unclear how individual T cells respond to these signaling pathways to make critical cell fate decisions. Here we reported that Uhrf1 was up-regulated and *Foxp3* methylation was increased upon TCR stimulation in naive T cells. *Uhrf1*$^{-/-}$ naive T cells underwent T reg cell–biased differentiation after TCR stimulation, which was correlated with enhanced expression and DNA hypomethylation of T reg cell–specific genes. Moreover, adoptive transfer of these *Uhrf1*$^{-/-}$ naive T cells could significantly suppress colitis. These results revealed an important role for Uhrf1: conventional T cells up-regulated Uhrf1 expression upon TCR stimulation, which maintained conventional T cell identity during activation and proliferation, thus maintaining immune homeostasis.

Many studies have revealed the critical role of TGF-β in inducing Foxp3 expression, and most of those studies focused on transcriptional regulation by the activation of Smad2/3, which occurs almost immediately after TGF-β treatment (Poncelet et al., 1999; Zi et al., 2011). However, the expression of *Foxp3* mRNA reached a high level after 48 h upon TGF-β stimulation (Ichiyama et al., 2008; Lu et al., 2010); this time lag between Foxp3 expression and Smad2/3 activation suggested that DNA demethylation may exist to initiate Foxp3 expression after TGF-β stimulation. In the current study, we found that *Uhrf1*$^{-/-}$ naive T cells could differentiate into phenotypically similar WT iT reg cells with TCR stimulation alone in the absence TGF-β, which suggested that TGF-β might induce iT reg cell differentiation by inhibiting Uhrf1 function. Indeed, Uhrf1 was observed to be phosphorylated upon TGF-β treatment and was mainly sequestered in the cytoplasm instead of the nucleus, where it performed the DNA methylation function and ultimately underwent proteasome-dependent degradation. As a consequence, the *Foxp3* promoter region underwent replication-coupled

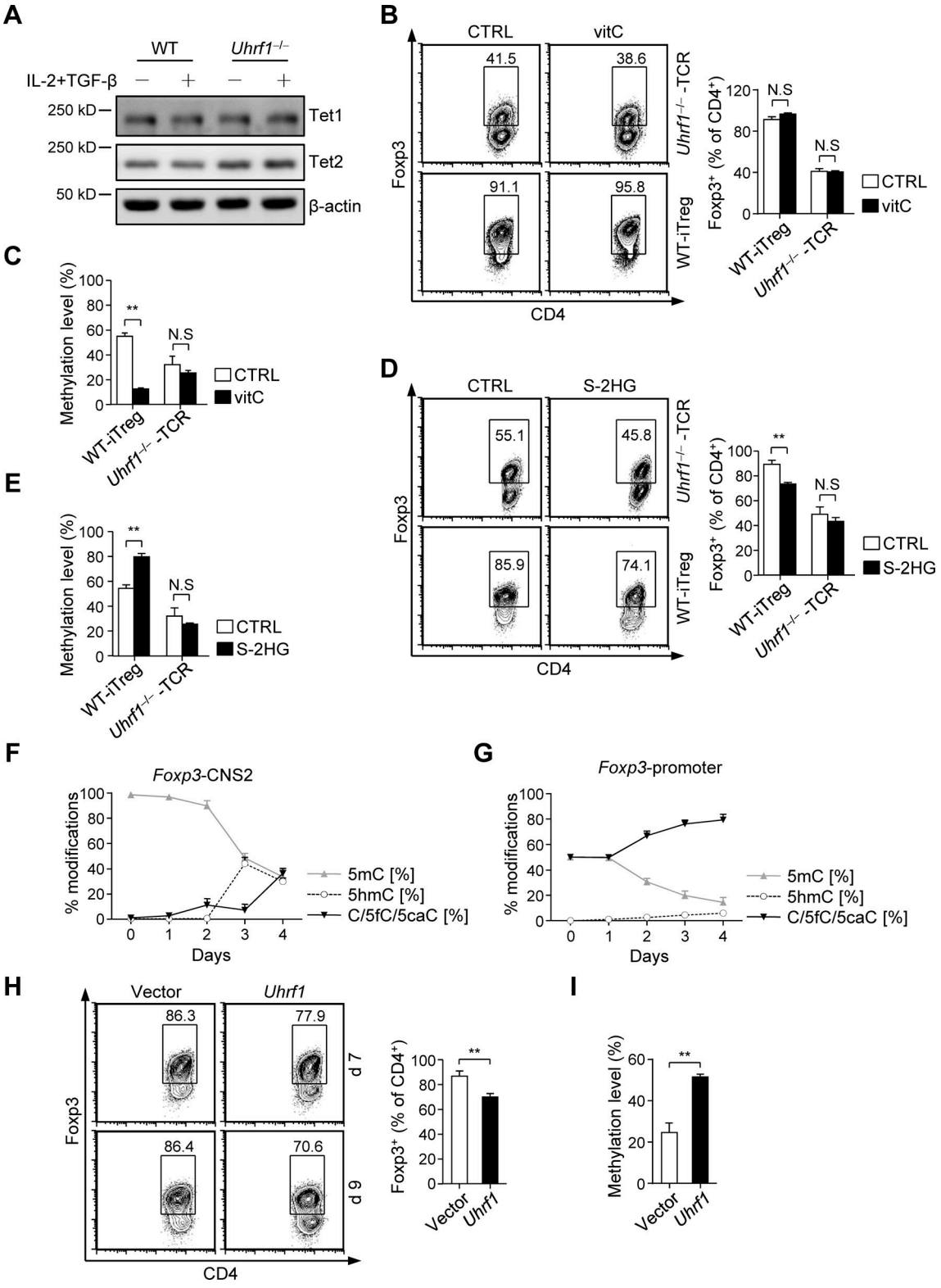

Figure 7. **Passive demethylation regulates Foxp3 induction during iT reg cell differentiation. (A)** Immunoblot analysis of Tet1 and Tet2 in WT and *Uhrf1*$^{-/-}$ naive T cells stimulated with anti-CD3 and anti-CD28 or cultured under iT reg skewing conditions for 3 d. **(B and D)** Flow-cytometric analysis of Foxp3 expression in WT and *Uhrf1*$^{-/-}$ naive T cells cultured under iT reg skewing condition or with anti-CD3 and anti-CD28 respectively, in the presence or absence of vitamin C (vitC; 10 µg/ml; B) and S-2HG (0.5 mM; E) for 4 d. Frequency of Foxp3^{+}CD4^{+} T cells was quantified (n = 3). CTRL, control. **(C and E)** The methylation levels of *Foxp3* promoter region in WT and *Uhrf1*$^{-/-}$ naive T cells treated as described in B or D (n = 3). **(F)** Percentages of 5-mC, 5-hmC, and C/5fC/5caC at the *Foxp3* CNS2 region of WT T cells cultured under iT reg cell skewing conditions (10 ng/ml IL-2 and 10 ng/ml TGF-β) for the indicated times (n = 3). **(G)** Percentages of 5-mC, 5-hmC, and C/5fC/5caC at the *Foxp3* promoter region of WT T cells cultured under iT reg cell skewing conditions (10 ng/ml IL-2 and 10 ng/ml TGF-β) for the indicated times (n = 3). **(H)** Flow-cytometric analysis of Foxp3 expression in WT naive T cells transfected with *Uhrf1* or vector and then cultured

under iT reg skewing conditions (10 ng/ml IL-2 and 10 ng/ml TGF-β) for 7 or 9 d. Frequency of Foxp3$^+$CD4$^+$ T cells was quantified (n = 3). **(I)** The methylation levels of *Foxp3* promoter region in WT T cells treated as described in H (n = 4). All data are shown as means ± SD; for all panels, **, P < 0.01, by Student's t test; N.S., no significance. All data are representative of or combined from at least three independent experiments.

dilution of 5-mC during cell division, which made the gene loci accessible for transcription factors to initiate its expression. Notably, after TGF-β signaling blockage, *Uhrf1*$^{-/-}$ T cells still showed increased Foxp3 expression upon TCR stimulation compared with WT T cells, although the expression was moderately lower than vehicle-treated *Uhrf1*$^{-/-}$ T cells. From these data, we thought TGF-β signaling might initiate Foxp3 induction in two processes. First, TGF-β could decrease *Foxp3* methylation via blocking Uhrf1 function. Second, when *Foxp3* locus was demethylated, TCR- and TGF-β–induced downstream factors might cooperatively promote *Foxp3* transcription, which was consistent with the previous reports that Smad protein and transcription factors could cooperate to induce Foxp3 expression through its enhancer (Chen et al., 2003; Tone et al., 2008; Ruan et al., 2009). These findings supported a unique epigenetic regulatory model to explain how TGF-β signaling promotes Foxp3 expression by modulating Uhrf1 activity.

The Uhrf1–Dnmt1 complex is well established to be indispensable for maintaining global DNA methylation following DNA replication (Qin et al., 2015). However, whether these two components are of equal importance and which component determines target specificity of DNA methylation during T cell differentiation are largely unknown. Here, our study found that Foxp3 expression was increased in *Uhrf1*$^{-/-}$ naive T cells with TCR stimulation alone, which was consistent with the phenotype of T cells deficient in Dnmt1 (Josefowicz et al., 2009). In addition, we also demonstrated that TGF-β regulated Uhrf1 translocation and induced its degradation to induce iT reg cell differentiation, whereas the expression of Dnmt1 was barely altered upon TGF-β stimulation. These findings revealed that although both Uhrf1 and Dnmt1 repressed Foxp3 expression by maintaining its methylation, only upstream Uhrf1 could respond to TGF-β signaling and determine the target specificity of DNA methylation during iT reg cell differentiation. In addition, we observed a distinct T reg cell–biased differentiation after Uhrf1 deletion, whereas the expression of cytokines was promiscuous in Dnmt1-deficient T cells (Lee et al., 2001; Makar and Wilson, 2004). This phenotypic difference suggested that DNA demethylation was sufficient to initiate Foxp3 transcription, while expression of cytokines might include other functions of Uhrf1, such as transcriptional regulation via chromatin modifications and ubiquitin ligase activity (Jenkins et al., 2005; Kim et al., 2009). Collectively, these findings suggested that despite the cooperation of Uhrf1 and Dnmt1 in DNA methylation maintenance, there was subtle difference between these two molecules, and Uhrf1 determined the target specificity of DNA methylation during iT reg cell differentiation, which made Uhrf1 a better therapeutic drug candidate of inflammatory diseases for generating stable iT reg cells.

In T reg cells, DNA demethylation of the *Foxp3* promoter and CNS2 region is important for inducing and stabilizing Foxp3 expression, and maintaining T reg cell identity (Kim and Leonard, 2007; Ohkura et al., 2012; Feng et al., 2014; Li et al., 2014). Moreover, disturbance of this fine-tuned epigenetic process can result in overt pathological consequences. It has been reported that TET-mediated active DNA demethylation maintains the demethylated status of CNS1 and CNS2 in the *Foxp3* locus and regulates the stability of Foxp3 expression (Yue et al., 2016). In the current study, we revealed that TGF-β regulated passive demethylation of the *Foxp3* promoter region and further Foxp3 expression during iT reg cell differentiation through suppressing Uhrf1 function. In addition, this passive DNA demethylation exerted its function during cell division upon TCR stimulation. Altogether, passive DNA demethylation involving Uhrf1 cooperated with TET-mediated active DNA demethylation to induce Foxp3 expression and control Foxp3 stability, respectively.

Uhrf1 has been reported to specifically facilitate the proliferation and maturation of colonic regulatory T cells but not the maintenance of extracolonic T reg cells, and *Uhrf1*$^{-/-}$ mice developed spontaneous colitis before 10 wk of age under specific pathogen–free (SPF) conditions, while they did not display any inflammation under germ-free conditions (Obata et al., 2014). Here we did not observe spontaneous colitis of *Uhrf1*$^{-/-}$ mice raised under SPF conditions. As differences in animal housing facilities and diet might affect study outcome (Hirayama et al., 1990; Reliene and Schiestl, 2006), we speculated the different environment between their and our animal facilities might determine whether or not spontaneous colitis occurred. In addition, Obata et al. (2014) found that Uhrf1 facilitated colonic T reg cell proliferation to restrain colitis, while our data demonstrated that Uhrf1 inhibited iT reg cell differentiation to keep the identity of conventional T cells. Notably, increasing evidence suggested that the same factors might play distinct roles in different T reg cell subsets (Pabbisetty et al., 2014; Kitagawa et al., 2017; Wu et al., 2017; Ghosh et al., 2018). Colonic T reg cells and iT reg cells were generated in different locations and in response to different environmental signals (Zhou et al., 2009; Josefowicz et al., 2012; Arpaia et al., 2013; Furusawa et al., 2013; Luu et al., 2017), and a single-cell transcriptomics study showed that T reg cells generated from lymphoid organs and colon were quite heterogeneous, which might be due to their adaptation to the local environments (Miragaia et al., 2019). In this context, Uhrf1 might exert distinct functions in different T reg cell subsets.

In summary, our study revealed a unique regulation of Uhrf1 in restraining T reg cell differentiation during conventional T cell activation and proliferation and demonstrated that TGF-β functioned to unleash this regulation via sequestering Uhrf1 in the cytoplasm. In addition, our study could broaden the underlying mechanisms by which TGF-β mediates T reg cell generation through regulating DNA methylation and may provide a novel potential therapeutic target in inflammatory diseases.

Materials and methods

Mice

All animal experiments were conducted according to the National Institutes of Health guidelines and were approved by the Institutional Animal Care and Use Committee of the Shanghai Institute of Biochemistry and Cell Biology, Chinese Academy of Sciences. The *Uhrf1*$^{fl/fl}$ mice were obtained as described (Cui et al., 2016) and were backcrossed for ≥10 generations with C57BL/6J. *Cd4*-Cre transgenic mice were obtained as described previously (Sun et al., 2014). CD45.1 mice (strain: B6.SJL-*Ptprc*^{a}*Pepc*^{b}/BoyJ) and *Rag1*$^{-/-}$ mice (strain: B6.129S7-*Rag1*^{tm1Mom}/J) were purchased from The Jackson Laboratory. Foxp3-EGFP mice (strain: B6.Cg-*Foxp3*^{tm2Tch}/J) were obtained from H.L. Wang (Shanghai Jiao Tong University School of Medicine, Shanghai, China). 6–10-wk-old sex-matched mice were used unless otherwise indicated. We used *Uhrf1*$^{fl/fl}$ littermates as WT mice. All the mice were bred in the SPF facility and genotyped by PCR before experimentation (*Uhrf1*-forward primer: 5′-CAGCCAGTG TTCTTAACCTCCAA-3′; *Uhrf1*-reverse primer: 5′-CTCCCACGT AACCCTAGATCCTT-3′).

Antibodies and reagents

The following antibodies from BD Biosciences were used: anti-CD4 (RM4-5), anti-CD8 (RPA-T8), anti-CD44 (IM7), anti-CD62L (MEL-14), anti-CD69 (H1.2F3), anti-CD45.2 (104), anti-CD45.1 (A20), anti–IL-4 (11B11), and anti-Smad2 (pS465/pS467)/Smad3 (pS423/pS425) (072–670). The following antibodies from BioLegend were used: anti-CD25 (PC61), anti-CD45RB (C363-16A), anti-IFN-γ (XMG1.2), and anti–IL-17A (TC11-18H10.1). The following antibodies were from eBioscience: anti-Foxp3 (FJK-16s), anti-Ki-67 (SolA15), and neutralized TGF-β antibody (16–9243-85). The following antibodies were from R&D Systems: anti-TβRI (FAB5871P), and anti-TβRII (FAB532P). Antibody against Dnmt1 (60B1220.1) was purchased from Novus Biologicals. Antibody against β-actin (ab40009) was purchased from Multi-Sciences. Antibodies against lamin B1 (sc-374015), α-tubulin (sc-23948), Ub (sc-8017), goat anti-rabbit IgG-HRP (sc-2004), and m-IgGκ BP-HRP (sc-516102) were purchased from Santa Cruz Biotechnology. Antibodies against phosphoserine (ab6639), Usp7 (ab157132), and Tet1 (ab191698) were purchased from Abcam. Antibody against Tet2 (21207–1-AP) was purchased from Proteintech. A homemade rabbit antibody directed against a glutathione-S-transferase fusion protein containing amino acids 594–701 of mouse Uhrf1 was derived using conventional methods (Leenaars and Hendriksen, 2005). Mimosine (M0253), hydroxyurea (H8627), collagenase D (11088866001), and DNase I (11284932001) were purchased from Sigma-Aldrich. Roscovitine and SB431542 were purchased from Selleck. Taq Master Mix was purchased from Vazyme Biotech.

Tissue lymphocyte preparation

Cells were isolated from spleens and lymph nodes by grinding with cell strainers. For cLP isolation, colons were excised and placed in cold PBS. After being minced into ∼0.5-cm pieces, the colons were incubated in RPMI 1640 medium (Gibco) containing 10 mM Hepes and 5 mM EDTA at 37°C for 20 min. The remaining tissues were further minced into ∼1-mm pieces, and digested with 5% FBS, 0.2 mg/ml collagenase D, and 0.1 mg/ml DNase I in RPMI 1640 medium for 1 h at 37°C with constant agitation. The resulting cell suspensions were filtered through a cell strainer (40 μM; BD Biosciences), and lymphocytes were purified on a 40%/70% Percoll (GE Healthcare) gradient by centrifugation.

Flow cytometry and sorting

Surface markers were stained in HBSS with 0.1% BSA for 30 min at 4°C (antibodies are listed above). For cytokine staining, cells were stimulated with 50 ng/ml PMA (Sigma-Aldrich) and 1 mg/ml ionomycin (Merck) in the presence of 1,000× brefeldin A (eBioscience) for 4 h at 37°C. Cells were first stained with antibodies against indicated cell surface markers followed by 10 min of fixation with 2% formaldehyde solution in PBS at room temperature and 5 min of permeabilization in Perm/Wash Buffer (BD Biosciences) at 4°C. For Foxp3 staining, cells were fixed and permeabilized with the Foxp3 Staining Buffer Set according to the manufacturer's instructions (eBioscience). To track cell division, T reg cells were labeled in vitro with CFSE (Sigma-Aldrich) or CellTrace Violet (Life Technologies) according to the manufacturer's protocol. Cell fluorescence was acquired on a four-laser BD LSR Fortessa II or a two-laser BD FACS Calibur and was analyzed with FlowJo software (TreeStar). Cell sorting was carried out by a BD FACSAria II after surface staining. Sorted cell purity was over 95%.

T cell purification and differentiation

Naive CD4^{+} T cells (CD4^{+}CD25^{-}CD44^{low}CD62L^{high}) were isolated from mouse total spleen and lymph node cells using the EasySep Mouse Naive CD4^{+} T Cell Isolation Kit (STEMCELL Technologies), following the manufacturer's instructions. For analysis of the in vitro T reg cell suppression assay, naive CD4^{+} T cells were sorted from CD45.1^{+} mice using a BD FACS Aria II Flow Cytometer. Isolated naive CD4^{+} T cells were stimulated for 4 d in 48-well flat-bottomed plates with plate-bound anti-CD3 and anti-CD28 (1 μg/ml each; BD Biosciences), β-mercaptoethanol (50 μM; Shanghai Genebase Gene-Tech), and 10% FBS in RPMI 1640 medium unless otherwise indicated. For iT reg skewing conditions, the cells were cultured in RPMI 1640 medium supplemented with recombinant murine IL-2 (10 ng/ml; PeproTech) and recombinant human TGF-β1 (10 ng/ml unless otherwise indicated; PeproTech). For Th1 cell condition, the cells were cultured in RPMI 1640 medium supplemented with recombinant murine IL-2 (10 ng/ml), recombinant murine IL-12 (10 ng/ml; PeproTech) and anti–IL-4 (10 μg/ml; BD Biosciences). For Th17 cell condition, the cells were cultured in RPMI 1640 medium supplemented with recombinant murine IL-6 (20 ng/ml; PeproTech), recombinant human TGF-β1 (5 ng/ml), recombinant murine IL-1β (10 ng/ml; PeproTech), recombinant murine IL-21 (50 ng/ml; PeproTech), recombinant human IL-23 (20 ng/ml; PeproTech), anti–IFN-γ (10 μg/ml; BD Biosciences), and anti–IL-4 (10 μg/ml; BD Biosciences).

In vitro T reg cell suppression assay

Sorted naive CD4^{+}CD25^{-}CD45RB^{high} T cells (6 × 10^{4} cells) were labeled with 5 μM CFSE for 10 min at 37°C and then cultured together with sorted WT nT reg cells (CD4^{+}GFP^{+}), WT iT reg cells

($CD4^+GFP^+$), or stimulated (anti-CD3 and anti-CD28) *Uhrf1*$^{-/-}$ T cells ($CD4^+GFP^+$) at the indicated ratio at 37°C in 200 µl of RPMI medium plus 10% FBS, supplemented with 50 µM β-mercaptoethanol in the presence of Dynabeads Mouse T-Activator CD3/CD28 (Thermo Fisher Scientific) in round-bottomed 96-well dishes. After 72 h, the cells were harvested, and CFSE dilution was measured by flow cytometry.

In vivo suppression assay and transfer model of colitis

Sorted naive $CD4^+CD25^-CD45RB^{high}$ T cells (5×10^5 per mouse) from CD45.1$^+$ mice in combination with WT or *Uhrf1*$^{-/-}$ T reg cells (5×10^5 per mouse) were i.v. injected into *Rag1*$^{-/-}$ recipient mice. Naive T cells were also transferred without T reg cells as a control group in the suppression assay. In the transfer model of colitis, naive $CD4^+CD25^-CD45RB^{high}$ T cells (5×10^5 per mouse) from WT or *Uhrf1*$^{-/-}$ mice were transferred to *Rag1*$^{-/-}$ mice by i.v. injection. The transferred mice were monitored daily for weight loss. The mice were euthanized when some mice reached a 20% reduction of initial weight, and colons and other lymphoid organs were collected for flow-cytometric analyses and H&E staining.

Histology staining

Mouse tissues were fixed in 10% formalin and stored in 70% ethanol until staining. Paraffin-embedded sections were cut and stained with H&E. Slides were then examined on an Olympus BX51 microscope.

Immunofluorescence

Confocal microscopy for Uhrf1 localization was performed as previously described (Zhao et al., 2017). Briefly, isolated naive T cells were stimulated with anti-CD3 and anti-CD28 in the presence or absence of TGF-β for indicated times. Cells were then harvested, fixed with 4% paraformaldehyde in PBS, and settled on coverslips coated with poly-L-lysine (Sigma-Aldrich) at 37°C for 1 h. Cells were permeabilized with 0.5% Triton X-100 and blocked with 1% BSA in Tris-buffered saline and Tween 20. Then cells were stained with Uhrf1 antibody diluted in blocking buffer (1:100), followed by incubation with secondary antibody conjugated to Cy3 (111–165-144; Jackson ImmunoResearch) together with DAPI (1 µg/ml; Cell Signaling Technology). Slides were analyzed on a Leica confocal microscope TCS SP8. ImageJ software was used to determine fluorescence intensity of pixels.

Cell culture and retroviral infections

The HEK293T cell line was purchased from the Cell Bank (Shanghai Institute of Biochemistry and Cell Biology, Chinese Academy of Sciences). The PlatE cell line was obtained from G. Pei (Shanghai Institute of Biochemistry and Cell Biology, Chinese Academy of Sciences, Shanghai, China) and was originally purchased from Cell Biolabs. The cells were cultured in a humidified incubator at 37°C with 5% CO_2 in DMEM (Gibco) supplemented with 10% FBS (Gibco) and 1% penicillin/streptomycin (Gibco).

cDNAs of mouse genes were cloned into the pMX-IRES-GFP retroviral vector. The virus was packaged in the PlatE cell line, and after transfection for 48 h, viral culture supernatants were harvested, supplemented with 8 µg/ml polybrene (Sigma-Aldrich), and added to previously stimulated T cells (1×10^6 per well, plate-bound anti-CD3 and anti-CD28 for 24 h). Then, the cells were centrifuged at 1,500 *g* for 2 h at 32°C. Retroviral supernatants were replaced with fresh RPMI culture medium with cytokines after transduction.

Immunoblot analysis and immunoprecipitation

Cells were lysed with 1× SDS sample buffer (50 mM Tris-HCl, pH 6.8, 100 mM dithiothreitol, 2% SDS, and 10% glycerol) and incubated at 95°C for 10 min. Proteins were separated by SDS-PAGE and transferred to nitrocellulose membranes (GE Healthcare). Membranes were incubated with 5% BSA in Tris-buffered saline and Tween 20 (0.5 M NaCl, Tris-HCl, pH 7.5, and 0.1% [vol/vol] Tween-20) for 60 min at room temperature. Proteins were detected with antibodies as described above. Membranes were visualized by immunoblot analysis with the enhanced chemiluminescence detection system (Thermo Fisher Scientific).

For immunoprecipitation, cells were lysed in lysis buffer (150 mM NaCl, 1% Triton X-100, 1 mM EDTA, and 50 mM Tris-HCl), supplemented with protease inhibitor cocktail, 1 mM NaF, and 1 mM Na_3VO_4. Cell lysates were incubated with the primary antibody-conjugated protein A/G beads (Santa Cruz Biotechnology) for 4–6 h at 4°C. Beads were washed extensively, and eluted with 1× SDS sample buffer. The eluates were subjected to immunoblot analysis and mass spectrometry.

ChIP assay

Purified naive T cells were stimulated with precoated anti-CD3 and anti-CD28 for 4 d, and ChIP assay was performed based on the manufacturer's instructions (Millipore). Briefly, stimulated WT and *Uhrf1*$^{-/-}$ naive T cells were cross-linked for 30 min on ice with 1% formaldehyde and lysed for 10 min on ice. The lysates were then sonicated to obtain DNA fragments of an average length of 500 bp. The fragmented lysates were subjected to immunoprecipitation with the indicated antibodies. The recovered DNA was used as templates for real-time PCR quantification. Data were normalized by input DNA for each sample. The following primers were used for quantitative PCR: *Foxp3* promoter forward primer: 5′-TTTCAGATGACTTGTAAAGGGCAAAG-3′; *Foxp3* promoter reverse primer: 5′-GAGTGTGTGTGCTGATAATTGCAGG-3′; *Foxp3* CNS2.2 forward primer: 5′-CCCTCTGGCATCCAAGAAAG-3′; *Foxp3* CNS2.2 reverse primer: 5′-GGGTGCTAGCGGATGTGGTA-3′; *Foxp3* CNS2.4 forward primer: 5′-CCCAACAGACAGTGCAGGAA-3′; and *Foxp3* CNS2.4 reverse primer: 5′-AAAGAGGACCTGAATTGGATATGG-3′.

Quantitative real-time PCR analysis

Total RNA was extracted from isolated or cultured T cells with TRIzol (Invitrogen), and reverse-transcribed with the SuperScript III First-Strand Synthesis System (Invitrogen). Real-time PCR was performed on the Rotor Gene 6000 machine (Corbett Life Sciences) with SYBR Green QPCR Master Mix (Toyobo). *GAPDH* was used as internal control. The sequences of quantative PCR primers for the genes examined are listed below:*Uhrf1* forward primer: 5′-CTGGCTATGGTGTGGGTCACAG-3′; *Uhrf1*

reverse primer: 5′-CTGGGCCTCAAACCATGCAC-3′; *Ifng* forward primer: 5′-GCGTCATTGAATCACACCTG-3′; *Ifng* reverse primer: 5′-ACCTGTGGGTTGTTGACCTC-3′; *Tbx21* forward primer: 5′-CAACAACCCCTTTGCCAAAG-3′; *Tbx21* reverse primer: 5′-TCCCCCAAGCAGTTGACAGT-3′; *IL4* forward primer: 5′-AGATGGATGTGCCAAACGTCCTCA-3′; *IL4* reverse primer: 5′-AATATGCGAAGCACCTTGGAAGCC-3′; *Gata3* forward primer: 5′-AGAACCGGCCCCTTATGAA-3′; *Gata3* reverse primer: 5′-AGTTCGCGCAGGATGTCC-3′; *Il17A* forward primer: 5′-GCTCCAGAAGGCCCTCAGACTA-3′; *Il17A* reverse primer: 5′-CAGGATCTCTTGCTGGATGAGAACAG-3′; *Rorc* forward primer: 5′-TTCACCCCACCTCCACTG-3′; *Rorc* reverse primer: 5′-GTGCAGGAGTAGGCCACATT-3′; *Foxp3* forward primer: 5′-GGCCCTTCTCCAGGACAGA-3′; *Foxp3* reverse primer: 5′-GCTGATCATGGCTGGGTTGT-3′; *Gapdh* forward primer: 5′-ACTCCACTCACGGCAAATTCA-3′; and *Gapdh* reverse primer: 5′-GCCTCACCCCATTTGATGTT-3′.

WGBS

WGBS was performed as previously described (Kulis et al., 2015; Zhang et al., 2017). Briefly, ∼5 µg genomic DNA was spiked with unmethylated 26 ng λ DNA. DNA was fragmented into 200–300 bp with Covaris S220 (Covaris), followed by end repair and adenylation. Then these DNA fragments were treated twice with bisulfite using the EZ DNA Methylation Gold Kit (Zymo Research). The resulting single-strand DNA fragments were PCR-amplificated using the KAPA HiFi HotStart Uracil + ReadyMix (2X; Kapa Biosystems). The library concentration was quantified by Qubit 2.0 Flurometer (Life Technologies) and quantitative PCR (iCycler, BioRad Laboratories), and the insert size was assayed on the Agilent Bioanalyzer 2100 system. The library preparations were sequenced on an Illumina Hiseq X Ten platform (Illumina) to generate 150 bp paired-end reads by the Novogene Bioinformatics Institute.

Bisulfite sequencing analysis

Bisulfite sequencing was started with 1×10^6 cells and converted with the EZ DNA Methylation-Direct Kit (Zymo Research). Selected genomic regions were PCR-amplified by the Taq HS enzyme (Takara). PCR products amplified from a DNA sample were recovered using the Gel Extraction Kit (Qiagen) and ligated into the pMD 18-T vector (Takara) for sequencing. Sequencing data were analyzed with BISMA (http://services.ibc.uni-stuttgart.de/BDPC/BISMA/).

The sequences of the *Foxp3* primer sets were as follows: promoter forward, 5′-GTGGTGAGGGGAAGAAATTATATTT-3′ and reverse, 5′-TAACACCCACCCTCAATACCTCT-3′; CNS2 forward, 5′-TTGGGTTTTTTTGGTATTTAAGAAAGA-3′ and reverse, 5′-CCCTATTATCACAACCTAAACTTAACCAA-3′.

RNA-seq, library generation, and bioinformatics analysis

RNA was extracted, purified, and checked for integrity using a RNA Nano 6000 Assay Kit of the Bioanalyzer 2100 system (Agilent Technologies). Libraries were generated for sequencing using NEBNext Ultra RNA Library Prep Kit for Illumina (NEB) following the manufacturer's recommendations. The library preparations were sequenced on an Illumina Hiseq platform, and 125 bp/150 bp paired-end reads were generated. The sequenced reads were aligned to the mouse genome (mm10) using HISAT2 (v2.0.5), and featureCounts (v1.5.0-p3) was used to count the reads numbers mapped to each gene. Fragments per kilobase per million mapped reads of each gene was calculated based on the length of the gene and reads count mapped to this gene. Differential expression analysis was performed using the DESeq2 R package (1.16.1). The P values were adjusted using the Benjamini and Hochberg method, and genes with an adjusted P value <0.05 found by DESeq2 were assigned as differentially expressed.

For GO enrichment analysis, selected differentially regulated genes between WT and *Uhrf1*$^{-/-}$ T cells with an adjusted P value <0.05 were analyzed by the GOseq R package.

Statistical analysis

Statistical analyses were performed with GraphPad Prism 6.0 (GraphPad). Unless indicated, all experiments shown were performed at least three times. All data are shown as means ± SD, and to compare the statistical significance of two independent groups, Student's *t* test was used to calculate P values unless otherwise indicated. For all experiments, *, $P < 0.05$; **, $P < 0.001$; ***, $P < 0.0001$; and N.S., no significance.

Data availability

All sequencing data that support the findings of this study have been deposited in the Gene Expression Omnibus of the National Center for Biotechnology Information under accession no. GSE128480.

Online supplemental material

Fig. S1 shows T cell development and GO enrichment analysis after Uhrf1 deletion. Fig. S2 shows effects of Uhrf1 deficiency on the expression of TGF-β receptors and effector T cell differentiation. Fig. S3 shows DNA methylation patterns and expression of Foxp3 in the absence of Uhrf1 and that maintenance of *Foxp3* methylation depends on the Uhrf1–Dnmt1 interaction. Fig. S4 shows that TGF-β signaling sequesters Uhrf1 in the cytoplasm. Fig. S5 shows regulation of Uhrf1 ubiquitination after TGF-β treatment.

Acknowledgments

We thank Baojin Wu and Guoyuan Chen for the animal husbandry and Wei Bian for the support of cell sorting.

This work was financially supported by the National Natural Science Foundation of China (31621003, 31530021, 91542122, and 31500717), and the Strategic Priority Research Program of the Chinese Academy of Sciences (XDB19000000).

The authors declare no competing financial interests.

Author contributions: X. Sun designed and performed most experiments, analyzed data, and prepared the manuscript. Y. Cui designed and performed experiments, and analyzed data. H. Feng performed the genotyping and plasmids construction experiments. H. Liu helped with mice construction and breeding. X. Liu conceptualized the research, directed the study, and prepared the manuscript.

Submitted: 27 March 2019
Revised: 28 July 2019
Accepted: 28 August 2019

References

Arpaia, N., C. Campbell, X. Fan, S. Dikiy, J. van der Veeken, P. deRoos, H. Liu, J.R. Cross, K. Pfeffer, P.J. Coffer, and A.Y. Rudensky. 2013. Metabolites produced by commensal bacteria promote peripheral regulatory T-cell generation. *Nature.* 504:451–455. https://doi.org/10.1038/nature12726

Au-Yeung, B.B., J. Zikherman, J.L. Mueller, J.F. Ashouri, M. Matloubian, D.A. Cheng, Y. Chen, K.M. Shokat, and A. Weiss. 2014. A sharp T-cell antigen receptor signaling threshold for T-cell proliferation. *Proc. Natl. Acad. Sci. USA.* 111:E3679–E3688. https://doi.org/10.1073/pnas.1413726111

Bilate, A.M., and J.J. Lafaille. 2012. Induced CD4+Foxp3+ regulatory T cells in immune tolerance. *Annu. Rev. Immunol.* 30:733–758. https://doi.org/10.1146/annurev-immunol-020711-075043

Bostick, M., J.K. Kim, P.O. Estève, A. Clark, S. Pradhan, and S.E. Jacobsen. 2007. UHRF1 plays a role in maintaining DNA methylation in mammalian cells. *Science.* 317:1760–1764. https://doi.org/10.1126/science.1147939

Chen, C., S. Zhai, L. Zhang, J. Chen, X. Long, J. Qin, J. Li, R. Huo, and X. Wang. 2018. Uhrf1 regulates germinal center B cell expansion and affinity maturation to control viral infection. *J. Exp. Med.* 215:1437–1448. https://doi.org/10.1084/jem.20171815

Chen, H., T. Yang, L. Zhu, and Y. Zhao. 2015. Cellular metabolism on T-cell development and function. *Int. Rev. Immunol.* 34:19–33. https://doi.org/10.3109/08830185.2014.902452

Chen, Q., Y.C. Kim, A. Laurence, G.A. Punkosdy, and E.M. Shevach. 2011. IL-2 controls the stability of Foxp3 expression in TGF-beta-induced Foxp3+ T cells in vivo. *J. Immunol.* 186:6329–6337. https://doi.org/10.4049/jimmunol.1100061

Chen, W., W. Jin, N. Hardegen, K.J. Lei, L. Li, N. Marinos, G. McGrady, and S.M. Wahl. 2003. Conversion of peripheral CD4+CD25- naive T cells to CD4+CD25+ regulatory T cells by TGF-beta induction of transcription factor Foxp3. *J. Exp. Med.* 198:1875–1886. https://doi.org/10.1084/jem.20030152

Chu, J., E.A. Loughlin, N.A. Gaur, S. SenBanerjee, V. Jacob, C. Monson, B. Kent, A. Oranu, Y. Ding, C. Ukomadu, and K.C. Sadler. 2012. UHRF1 phosphorylation by cyclin A2/cyclin-dependent kinase 2 is required for zebrafish embryogenesis. *Mol. Biol. Cell.* 23:59–70. https://doi.org/10.1091/mbc.e11-06-0487

Ciechanover, A. 2005. Proteolysis: from the lysosome to ubiquitin and the proteasome. *Nat. Rev. Mol. Cell Biol.* 6:79–87. https://doi.org/10.1038/nrm1552

Cui, Y., X. Chen, J. Zhang, X. Sun, H. Liu, L. Bai, C. Xu, and X. Liu. 2016. Uhrf1 Controls iNKT Cell Survival and Differentiation through the Akt-mTOR Axis. *Cell Reports.* 15:256–263. https://doi.org/10.1016/j.celrep.2016.03.016

Curotto de Lafaille, M.A., and J.J. Lafaille. 2009. Natural and adaptive foxp3+ regulatory T cells: more of the same or a division of labor? *Immunity.* 30:626–635. https://doi.org/10.1016/j.immuni.2009.05.002

Derynck, R., and Y.E. Zhang. 2003. Smad-dependent and Smad-independent pathways in TGF-beta family signalling. *Nature.* 425:577–584. https://doi.org/10.1038/nature02006

Dias, S., A. D'Amico, E. Cretney, Y. Liao, J. Tellier, C. Bruggeman, F.F. Almeida, J. Leahy, G.T. Belz, G.K. Smyth, et al. 2017. Effector Regulatory T Cell Differentiation and Immune Homeostasis Depend on the Transcription Factor Myb. *Immunity.* 46:78–91. https://doi.org/10.1016/j.immuni.2016.12.017

Feng, Y., A. Arvey, T. Chinen, J. van der Veeken, G. Gasteiger, and A.Y. Rudensky. 2014. Control of the inheritance of regulatory T cell identity by a cis element in the Foxp3 locus. *Cell.* 158:749–763. https://doi.org/10.1016/j.cell.2014.07.031

Floess, S., J. Freyer, C. Siewert, U. Baron, S. Olek, J. Polansky, K. Schlawe, H.D. Chang, T. Bopp, E. Schmitt, et al. 2007. Epigenetic control of the foxp3 locus in regulatory T cells. *PLoS Biol.* 5:e38. https://doi.org/10.1371/journal.pbio.0050038

Fontenot, J.D., M.A. Gavin, and A.Y. Rudensky. 2003. Foxp3 programs the development and function of CD4+CD25+ regulatory T cells. *Nat. Immunol.* 4:330–336. https://doi.org/10.1038/ni904

Furusawa, Y., Y. Obata, S. Fukuda, T.A. Endo, G. Nakato, D. Takahashi, Y. Nakanishi, C. Uetake, K. Kato, T. Kato, et al. 2013. Commensal microbe-derived butyrate induces the differentiation of colonic regulatory T cells. *Nature.* 504:446–450. https://doi.org/10.1038/nature12721

Ghosh, S., S. Roy-Chowdhuri, K. Kang, S.H. Im, and D. Rudra. 2018. The transcription factor Foxp1 preserves integrity of an active Foxp3 locus in extrathymic Treg cells. *Nat. Commun.* 9:4473. https://doi.org/10.1038/s41467-018-07018-y

Haribhai, D., J.B. Williams, S. Jia, D. Nickerson, E.G. Schmitt, B. Edwards, J. Ziegelbauer, M. Yassai, S.H. Li, L.M. Relland, et al. 2011. A requisite role for induced regulatory T cells in tolerance based on expanding antigen receptor diversity. *Immunity.* 35:109–122. https://doi.org/10.1016/j.immuni.2011.03.029

Hirayama, K., K. Endo, S. Kawamura, and T. Mitsuoka. 1990. Comparison of the intestinal bacteria in specific pathogen free mice from different breeders. *Jikken Dobutsu.* 39:263–267.

Hori, S., T. Nomura, and S. Sakaguchi. 2003. Control of regulatory T cell development by the transcription factor Foxp3. *Science.* 299:1057–1061. https://doi.org/10.1126/science.1079490

Huehn, J., and M. Beyer. 2015. Epigenetic and transcriptional control of Foxp3+ regulatory T cells. *Semin. Immunol.* 27:10–18. https://doi.org/10.1016/j.smim.2015.02.002

Hunter, T. 2007. The age of crosstalk: phosphorylation, ubiquitination, and beyond. *Mol. Cell.* 28:730–738. https://doi.org/10.1016/j.molcel.2007.11.019

Ichiyama, K., H. Yoshida, Y. Wakabayashi, T. Chinen, K. Saeki, M. Nakaya, G. Takaesu, S. Hori, A. Yoshimura, and T. Kobayashi. 2008. Foxp3 inhibits RORgammat-mediated IL-17A mRNA transcription through direct interaction with RORgammat. *J. Biol. Chem.* 283:17003–17008. https://doi.org/10.1074/jbc.M801286200

Jelley-Gibbs, D.M., N.M. Lepak, M. Yen, and S.L. Swain. 2000. Two distinct stages in the transition from naive CD4 T cells to effectors, early antigen-dependent and late cytokine-driven expansion and differentiation. *J. Immunol.* 165:5017–5026. https://doi.org/10.4049/jimmunol.165.9.5017

Jenkins, Y., V. Markovtsov, W. Lang, P. Sharma, D. Pearsall, J. Warner, C. Franci, B. Huang, J. Huang, G.C. Yam, et al. 2005. Critical role of the ubiquitin ligase activity of UHRF1, a nuclear RING finger protein, in tumor cell growth. *Mol. Biol. Cell.* 16:5621–5629. https://doi.org/10.1091/mbc.e05-03-0194

Johanns, T.M., J.M. Ertelt, J.H. Rowe, and S.S. Way. 2010. Regulatory T cell suppressive potency dictates the balance between bacterial proliferation and clearance during persistent Salmonella infection. *PLoS Pathog.* 6:e1001043. https://doi.org/10.1371/journal.ppat.1001043

Josefowicz, S.Z., C.B. Wilson, and A.Y. Rudensky. 2009. Cutting edge: TCR stimulation is sufficient for induction of Foxp3 expression in the absence of DNA methyltransferase 1. *J. Immunol.* 182:6648–6652. https://doi.org/10.4049/jimmunol.0803320

Josefowicz, S.Z., L.F. Lu, and A.Y. Rudensky. 2012. Regulatory T cells: mechanisms of differentiation and function. *Annu. Rev. Immunol.* 30:531–564. https://doi.org/10.1146/annurev.immunol.25.022106.141623

Kanamori, M., H. Nakatsukasa, M. Okada, Q. Lu, and A. Yoshimura. 2016. Induced Regulatory T Cells: Their Development, Stability, and Applications. *Trends Immunol.* 37:803–811. https://doi.org/10.1016/j.it.2016.08.012

Kent, B., E. Magnani, M.J. Walsh, and K.C. Sadler. 2016. UHRF1 regulation of Dnmt1 is required for pre-gastrula zebrafish development. *Dev. Biol.* 412:99–113. https://doi.org/10.1016/j.ydbio.2016.01.036

Kim, H.P., and W.J. Leonard. 2007. CREB/ATF-dependent T cell receptor-induced FoxP3 gene expression: a role for DNA methylation. *J. Exp. Med.* 204:1543–1551. https://doi.org/10.1084/jem.20070109

Kim, J.K., P.O. Estève, S.E. Jacobsen, and S. Pradhan. 2009. UHRF1 binds G9a and participates in p21 transcriptional regulation in mammalian cells. *Nucleic Acids Res.* 37:493–505. https://doi.org/10.1093/nar/gkn961

Kitagawa, Y., N. Ohkura, Y. Kidani, A. Vandenbon, K. Hirota, R. Kawakami, K. Yasuda, D. Motooka, S. Nakamura, M. Kondo, et al. 2017. Guidance of regulatory T cell development by Satb1-dependent super-enhancer establishment. *Nat. Immunol.* 18:173–183. https://doi.org/10.1038/ni.3646

Kulis, M., A. Merkel, S. Heath, A.C. Queirós, R.P. Schuyler, G. Castellano, R. Beekman, E. Raineri, A. Esteve, G. Clot, et al. 2015. Whole-genome fingerprint of the DNA methylome during human B cell differentiation. *Nat. Genet.* 47:746–756. https://doi.org/10.1038/ng.3291

Lal, G., N. Zhang, W. van der Touw, Y. Ding, W. Ju, E.P. Bottinger, S.P. Reid, D.E. Levy, and J.S. Bromberg. 2009. Epigenetic regulation of Foxp3 expression in regulatory T cells by DNA methylation. *J. Immunol.* 182:259–273. https://doi.org/10.4049/jimmunol.182.1.259

Lee, W., and G.R. Lee. 2018. Transcriptional regulation and development of regulatory T cells. *Exp. Mol. Med.* 50:e456. https://doi.org/10.1038/emm.2017.313

Lee, P.P., D.R. Fitzpatrick, C. Beard, H.K. Jessup, S. Lehar, K.W. Makar, M. Pérez-Melgosa, M.T. Sweetser, M.S. Schlissel, S. Nguyen, et al. 2001. A critical role for Dnmt1 and DNA methylation in T cell development,

function, and survival. *Immunity*. 15:763–774. https://doi.org/10.1016/S1074-7613(01)00227-8

Leenaars, M., and C.F. Hendriksen. 2005. Critical steps in the production of polyclonal and monoclonal antibodies: evaluation and recommendations. *ILAR J.* 46:269–279. https://doi.org/10.1093/ilar.46.3.269

Li, X., Y. Liang, M. LeBlanc, C. Benner, and Y. Zheng. 2014. Function of a Foxp3 cis-element in protecting regulatory T cell identity. *Cell*. 158:734–748. https://doi.org/10.1016/j.cell.2014.07.030

Liang, C.C., B. Zhan, Y. Yoshikawa, W. Haas, S.P. Gygi, and M.A. Cohn. 2015. UHRF1 is a sensor for DNA interstrand crosslinks and recruits FANCD2 to initiate the Fanconi anemia pathway. *Cell Reports*. 10:1947–1956. https://doi.org/10.1016/j.celrep.2015.02.053

Liang, G., M.F. Chan, Y. Tomigahara, Y.C. Tsai, F.A. Gonzales, E. Li, P.W. Laird, and P.A. Jones. 2002. Cooperativity between DNA methyltransferases in the maintenance methylation of repetitive elements. *Mol. Cell. Biol.* 22:480–491. https://doi.org/10.1128/MCB.22.2.480-491.2002

Liu, X., Q. Gao, P. Li, Q. Zhao, J. Zhang, J. Li, H. Koseki, and J. Wong. 2013. UHRF1 targets DNMT1 for DNA methylation through cooperative binding of hemi-methylated DNA and methylated H3K9. *Nat. Commun.* 4:1563. https://doi.org/10.1038/ncomms2562

Losman, J.A., R.E. Looper, P. Koivunen, S. Lee, R.K. Schneider, C. McMahon, G.S. Cowley, D.E. Root, B.L. Ebert, and W.G. Kaelin Jr. 2013. (R)-2-hydroxyglutarate is sufficient to promote leukemogenesis and its effects are reversible. *Science*. 339:1621–1625. https://doi.org/10.1126/science.1231677

Lu, L., J. Ma, X. Wang, J. Wang, F. Zhang, J. Yu, G. He, B. Xu, D.D. Brand, D.A. Horwitz, et al. 2010. Synergistic effect of TGF-β superfamily members on the induction of Foxp3+ Treg. *Eur. J. Immunol.* 40:142–152. https://doi.org/10.1002/eji.200939618

Luu, M., U. Steinhoff, and A. Visekruna. 2017. Functional heterogeneity of gut-resident regulatory T cells. *Clin. Transl. Immunology*. 6:e156. https://doi.org/10.1038/cti.2017.39

Ma, H., H. Chen, X. Guo, Z. Wang, M.E. Sowa, L. Zheng, S. Hu, P. Zeng, R. Guo, J. Diao, et al. 2012. M phase phosphorylation of the epigenetic regulator UHRF1 regulates its physical association with the deubiquitylase USP7 and stability. *Proc. Natl. Acad. Sci. USA*. 109:4828–4833. https://doi.org/10.1073/pnas.1116349109

Makar, K.W., and C.B. Wilson. 2004. DNA methylation is a nonredundant repressor of the Th2 effector program. *J. Immunol.* 173:4402–4406. https://doi.org/10.4049/jimmunol.173.7.4402

Marie, J.C., J.J. Letterio, M. Gavin, and A.Y. Rudensky. 2005. TGF-beta1 maintains suppressor function and Foxp3 expression in CD4+CD25+ regulatory T cells. *J. Exp. Med.* 201:1061–1067. https://doi.org/10.1084/jem.20042276

Miragaia, R.J., T. Gomes, A. Chomka, L. Jardine, A. Riedel, A.N. Hegazy, N. Whibley, A. Tucci, X. Chen, I. Lindeman, et al. 2019. Single-Cell Transcriptomics of Regulatory T Cells Reveals Trajectories of Tissue Adaptation. *Immunity*. 50:493–504.e7.

Mudbhary, R., Y. Hoshida, Y. Chernyavskaya, V. Jacob, A. Villanueva, M.I. Fiel, X. Chen, K. Kojima, S. Thung, R.T. Bronson, et al. 2014. UHRF1 overexpression drives DNA hypomethylation and hepatocellular carcinoma. *Cancer Cell*. 25:196–209. https://doi.org/10.1016/j.ccr.2014.01.003

Nardozzi, J.D., K. Lott, and G. Cingolani. 2010. Phosphorylation meets nuclear import: a review. *Cell Commun. Signal.* 8:32. https://doi.org/10.1186/1478-811X-8-32

Nguyen, L.K., W. Kolch, and B.N. Kholodenko. 2013. When ubiquitination meets phosphorylation: a systems biology perspective of EGFR/MAPK signalling. *Cell Commun. Signal.* 11:52. https://doi.org/10.1186/1478-811X-11-52

Obata, Y., Y. Furusawa, T.A. Endo, J. Sharif, D. Takahashi, K. Atarashi, M. Nakayama, S. Onawa, Y. Fujimura, M. Takahashi, et al. 2014. The epigenetic regulator Uhrf1 facilitates the proliferation and maturation of colonic regulatory T cells. *Nat. Immunol.* 15:571–579. https://doi.org/10.1038/ni.2886

Ohkura, N., M. Hamaguchi, H. Morikawa, K. Sugimura, A. Tanaka, Y. Ito, M. Osaki, Y. Tanaka, R. Yamashita, N. Nakano, et al. 2012. T cell receptor stimulation-induced epigenetic changes and Foxp3 expression are independent and complementary events required for Treg cell development. *Immunity*. 37:785–799. https://doi.org/10.1016/j.immuni.2012.09.010

Ohkura, N., Y. Kitagawa, and S. Sakaguchi. 2013. Development and maintenance of regulatory T cells. *Immunity*. 38:414–423. https://doi.org/10.1016/j.immuni.2013.03.002

Pabbisetty, S.K., W. Rabacal, D. Maseda, D. Cendron, P.L. Collins, K.L. Hoek, V.V. Parekh, T.M. Aune, and E. Sebzda. 2014. KLF2 is a rate-limiting transcription factor that can be targeted to enhance regulatory T-cell production. *Proc. Natl. Acad. Sci. USA*. 111:9579–9584. https://doi.org/10.1073/pnas.1323493111

Poncelet, A.C., M.P. de Caestecker, and H.W. Schnaper. 1999. The transforming growth factor-beta/SMAD signaling pathway is present and functional in human mesangial cells. *Kidney Int.* 56:1354–1365. https://doi.org/10.1046/j.1523-1755.1999.00680.x

Qin, W., H. Leonhardt, and F. Spada. 2011. Usp7 and Uhrf1 control ubiquitination and stability of the maintenance DNA methyltransferase Dnmt1. *J. Cell. Biochem.* 112:439–444. https://doi.org/10.1002/jcb.22998

Qin, W., P. Wolf, N. Liu, S. Link, M. Smets, F. La Mastra, I. Forné, G. Pichler, D. Hörl, K. Fellinger, et al. 2015. DNA methylation requires a DNMT1 ubiquitin interacting motif (UIM) and histone ubiquitination. *Cell Res.* 25:911–929. https://doi.org/10.1038/cr.2015.72

Razin, A., and B. Kantor. 2005. DNA methylation in epigenetic control of gene expression. *Prog. Mol. Subcell. Biol.* 38:151–167. https://doi.org/10.1007/3-540-27310-7_6

Reliene, R., and R.H. Schiestl. 2006. Differences in animal housing facilities and diet may affect study outcomes-a plea for inclusion of such information in publications. *DNA Repair (Amst.)*. 5:651–653. https://doi.org/10.1016/j.dnarep.2006.02.001

Ruan, Q., V. Kameswaran, Y. Tone, L. Li, H.C. Liou, M.I. Greene, M. Tone, and Y.H.H. Chen. 2009. Development of Foxp3(+) regulatory t cells is driven by the c-Rel enhanceosome. *Immunity*. 31:932–940. https://doi.org/10.1016/j.immuni.2009.10.006

Schlenner, S.M., B. Weigmann, Q. Ruan, Y. Chen, and H. von Boehmer. 2012. Smad3 binding to the foxp3 enhancer is dispensable for the development of regulatory T cells with the exception of the gut. *J. Exp. Med.* 209:1529–1535. https://doi.org/10.1084/jem.20112646

Selvaraj, R.K., and T.L. Geiger. 2007. A kinetic and dynamic analysis of Foxp3 induced in T cells by TGF-beta. *J. Immunol.* 178:7667–7677. https://doi.org/10.4049/jimmunol.178.12.7667

Sharif, J., M. Muto, S. Takebayashi, I. Suetake, A. Iwamatsu, T.A. Endo, J. Shinga, Y. Mizutani-Koseki, T. Toyoda, K. Okamura, et al. 2007. The SRA protein Np95 mediates epigenetic inheritance by recruiting Dnmt1 to methylated DNA. *Nature*. 450:908–912. https://doi.org/10.1038/nature06397

Sidhu, H., and N. Capalash. 2017. UHRF1: The key regulator of epigenetics and molecular target for cancer therapeutics. *Tumour Biol.* 39:1010428317692205. https://doi.org/10.1177/1010428317692205

Someya, K., H. Nakatsukasa, M. Ito, T. Kondo, K.I. Tateda, T. Akanuma, I. Koya, T. Sanosaka, J. Kohyama, Y.I. Tsukada, et al. 2017. Improvement of Foxp3 stability through CNS2 demethylation by TET enzyme induction and activation. *Int. Immunol.* 29:365–375. https://doi.org/10.1093/intimm/dxx049

Souchelnytskyi, S., K. Tamaki, U. Engström, C. Wernstedt, P. ten Dijke, and C.H. Heldin. 1997. Phosphorylation of Ser465 and Ser467 in the C terminus of Smad2 mediates interaction with Smad4 and is required for transforming growth factor-beta signaling. *J. Biol. Chem.* 272:28107–28115. https://doi.org/10.1074/jbc.272.44.28107

Sun, Y., X. Zhu, X. Chen, H. Liu, Y. Xu, Y. Chu, G. Wang, and X. Liu. 2014. The mediator subunit Med23 contributes to controlling T-cell activation and prevents autoimmunity. *Nat. Commun.* 5:5225. https://doi.org/10.1038/ncomms6225

Tian, Y., M. Paramasivam, G. Ghosal, D. Chen, X. Shen, Y. Huang, S. Akhter, R. Legerski, J. Chen, M.M. Seidman, et al. 2015. UHRF1 contributes to DNA damage repair as a lesion recognition factor and nuclease scaffold. *Cell Reports*. 10:1957–1966. https://doi.org/10.1016/j.celrep.2015.03.038

Tone, Y., K. Furuuchi, Y. Kojima, M.L. Tykocinski, M.I. Greene, and M. Tone. 2008. Smad3 and NFAT cooperate to induce Foxp3 expression through its enhancer. *Nat. Immunol.* 9:194–202. https://doi.org/10.1038/ni1549

Trerotola, M., V. Relli, P. Simeone, and S. Alberti. 2015. Epigenetic inheritance and the missing heritability. *Hum. Genomics*. 9:17. https://doi.org/10.1186/s40246-015-0041-3

Wieczorek, G., A. Asemissen, F. Model, I. Turbachova, S. Floess, V. Liebenberg, U. Baron, D. Stauch, K. Kotsch, J. Pratschke, et al. 2009. Quantitative DNA methylation analysis of FOXP3 as a new method for counting regulatory T cells in peripheral blood and solid tissue. *Cancer Res.* 69:599–608. https://doi.org/10.1158/0008-5472.CAN-08-2361

Williams, L.M., and A.Y. Rudensky. 2007. Maintenance of the Foxp3-dependent developmental program in mature regulatory T cells requires continued expression of Foxp3. *Nat. Immunol.* 8:277–284. https://doi.org/10.1038/ni1437

Workman, C.J., A.L. Szymczak-Workman, L.W. Collison, M.R. Pillai, and D.A. Vignali. 2009. The development and function of regulatory

T cells. *Cell. Mol. Life Sci.* 66:2603–2622. https://doi.org/10.1007/s00018-009-0026-2

Wu, C., Z. Chen, V. Dardalhon, S. Xiao, T. Thalhamer, M. Liao, A. Madi, R.F. Franca, T. Han, M. Oukka, and V. Kuchroo. 2017. The transcription factor musculin promotes the unidirectional development of peripheral T_{reg} cells by suppressing the T_H2 transcriptional program. *Nat. Immunol.* 18:344–353. https://doi.org/10.1038/ni.3667

Yue, X., S. Trifari, T. Äijö, A. Tsagaratou, W.A. Pastor, J.A. Zepeda-Martínez, C.W.J. Lio, X. Li, Y. Huang, P. Vijayanand, et al. 2016. Control of Foxp3 stability through modulation of TET activity. *J. Exp. Med.* 213:377–397. https://doi.org/10.1084/jem.20151438

Zhang, S., C. Qin, G. Cao, L. Guo, C. Feng, and W. Zhang. 2017. Genome-wide analysis of DNA methylation profiles in a senescence-accelerated mouse prone 8 brain using whole-genome bisulfite sequencing. *Bioinformatics.* 33:1591–1595.

Zhang, Z.M., S.B. Rothbart, D.F. Allison, Q. Cai, J.S. Harrison, L. Li, Y. Wang, B.D. Strahl, G.G. Wang, and J. Song. 2015. An Allosteric Interaction Links USP7 to Deubiquitination and Chromatin Targeting of UHRF1. *Cell Reports.* 12:1400–1406. https://doi.org/10.1016/j.celrep.2015.07.046

Zhao, J., X. Chen, G. Song, J. Zhang, H. Liu, and X. Liu. 2017. Uhrf1 controls the self-renewal versus differentiation of hematopoietic stem cells by epigenetically regulating the cell-division modes. *Proc. Natl. Acad. Sci. USA.* 114:E142–E151. https://doi.org/10.1073/pnas.1612967114

Zheng, Y., S. Josefowicz, A. Chaudhry, X.P. Peng, K. Forbush, and A.Y. Rudensky. 2010. Role of conserved non-coding DNA elements in the Foxp3 gene in regulatory T-cell fate. *Nature.* 463:808–812. https://doi.org/10.1038/nature08750

Zhou, L., M.M. Chong, and D.R. Littman. 2009. Plasticity of CD4+ T cell lineage differentiation. *Immunity.* 30:646–655. https://doi.org/10.1016/j.immuni.2009.05.001

Zi, Z., Z. Feng, D.A. Chapnick, M. Dahl, D. Deng, E. Klipp, A. Moustakas, and X. Liu. 2011. Quantitative analysis of transient and sustained transforming growth factor-β signaling dynamics. *Mol. Syst. Biol.* 7:492. https://doi.org/10.1038/msb.2011.22